

Mechanical pressure and momentum conservation in dry active matter

Y. Fily

Martin Fisher School of Physics, Brandeis University, Waltham, MA 02453, USA

Y. Kafri

Department of Physics, Technion, Haifa 32000, Israel

A. Solon

Department of Physics, Massachusetts Institute of Technology, Cambridge, Massachusetts 02139, USA

J. Tailleur[‡]

Université Paris Diderot, Sorbonne Paris Cité, MSC, UMR 7057 CNRS, 75205 Paris, France

A. Turner

Department of Physics, Technion, Haifa 32000, Israel

Abstract. We relate the breakdown of equations of states (EOS) for the mechanical pressure of generic dry active systems to the lack of momentum conservation in such systems. We show how net sources and sinks of momentum arise generically close to confining walls. These typically depend on the interactions of the container with the particles, which makes the mechanical pressure a container-dependent quantity. We show that an EOS is recovered if the dynamics of the propulsive forces of the particles are decoupled from other degrees of freedom and lead to an apolar bulk steady-state. This recovery of an EOS stems from the mean steady-state active force density being the divergence of the flux of “active impulse”, an observable which measures the mean momentum particles will receive from the substrate in the future.

[‡] Invited author

Contents

1	Noninteracting active particles	5
1.1	The Model	6
1.2	Momentum and Pressure	7
1.3	The breakdown of the EOS: momentum sources and sinks	9
1.4	Numerical measurement of sources and sinks	11
1.5	Torque-free active gas: active impulse and the emergence of an equation of state	12
1.6	Active impulse and swim pressure	18
1.7	Effective steady-state momentum conservation	18
2	Interacting active particles	20
2.1	Quorum sensing	22
2.2	Pairwise forces	23
3	Momentum sources in motility induced phase separation	24
3.1	Pairwise forces	25
3.2	Quorum sensing	26
4	Conclusion	28
Appendix A Sufficient condition for the existence of an equation of state		29
Appendix A.1	Example with multiplicative noise	32

Active particles convert energy stored in the environment into self-propelling mechanical forces. They have attracted a lot of interest in recent years [1] because of their broad applicability to model systems ranging from biological [2] through granular [3, 4], to colloidal systems [5–7]. They also hold tremendous promise for making great micro-scale machines [8]. A key aspect of designing such machines is predicting the mechanical pressure an active system exerts on its boundaries, a topic that is attracting much theoretical interest [9–26].

In standard thermodynamics, the pressure obeys an equation of state (EOS): it only depends on the bulk properties of the system and is independent of its boundary conditions. This has many implications. Consider for example a cavity filled with a fluid and separated into two halves by a mobile piston. The piston can only be set in motion if the fluids on each side have different bulk properties (e.g. densities or temperatures). This in turn constrains engine designs.

In contrast, we recently showed [13] that the pressure exerted by an active fluid on a flat wall need not obey an EOS. It generally depends explicitly on the potential describing the wall. Coming back to our container separated in two parts by a mobile piston, motion can now arise even when the fluids on both sides of the piston have the same bulk properties, provided the piston’s surfaces are different [13]. This wall dependence has since been shown experimentally in shaken granular systems [26]. Importantly, Refs. [13] and [26] deal with so-called *dry active systems*, i.e., systems that do not obey detailed balance (as is generically the case for active systems) and have no local momentum conservation (by pushing on a substrate or surrounding medium which acts as a momentum sink).

Note, however, that some dry active systems have been shown to admit an EOS [9, 11, 13, 14]. The role of pressure in such systems then shares similarities with its role in standard thermodynamics: for instance, it is equal in coexisting phases [14]. It can also be used to define an isobaric ensemble and hence to control active systems [27]. However, this link to equilibrium physics is only partial and, for instance, the Maxwell construction in the pressure-volume phase diagram does not yield the correct binodals in phase-separating active systems [14].

The goal of this paper is to relate the lack of EOS to a violation of momentum conservation. To do so, we revisit the results of Ref. [13] for a class of microscopic models of active particles that explicitly

account for their translational inertia, instead of studying the commonly used overdamped models. (Our previous results are then naturally recovered in the large damping limit.).

To help contextualize our results and state them more accurately, it is useful to first consider an equilibrium system and then a system (at equilibrium or not) with local momentum conservation. In the former, the extensivity of the free energy alone ensures the pressure only depends on bulk properties. In the latter, the momentum density field \mathbf{p} obeys the conservation equation [28]

$$\partial_t \mathbf{p} = -\nabla \cdot \mathbf{J}_{\mathbf{p}} . \quad (1)$$

Here $\mathbf{J}_{\mathbf{p}}$ is a tensorial current associated with the local conservation law for the momentum density (the flow of momentum for non-interacting particles). In the presence of an external wall, interacting with the particles through a potential V_{ext} , momentum can be exchanged with the system and the dynamics (1) becomes

$$\partial_t \mathbf{p} = -\nabla \cdot \mathbf{J}_{\mathbf{p}} - \rho \nabla V_{\text{ext}} , \quad (2)$$

where ρ is the particle density. The last term describes the exchange of momentum with the wall. Assuming for simplicity that the wall is flat and oriented normal to the x -direction (see Fig. 1), the pressure exerted on the wall is simply given by

$$P = \int_{x_b}^{\infty} dx \rho \partial_x V_{\text{ext}}(x) \quad (3)$$

where x_b refers to a point in the bulk, far away from the wall. Eqs. (2)-(3) are exact provided ρ , \mathbf{p} , and $\mathbf{J}_{\mathbf{p}}$ are understood as local statistical averages of the underlying instantaneous fields. At steady-state, substituting (2) into (3) readily yields $P = \left(\mathbf{J}_{\mathbf{p}}^{xx} \right)_{x=x_b}$. Assuming that the walls have no influence on the properties of the fluid in the bulk of the system, $\left(\mathbf{J}_{\mathbf{p}}^{xx} \right)_{x=x_b}$ is independent of the choice of x_b and P is a bulk property, independent of the specific wall potential V_{ext} .

In dry active systems, the self-propulsion force acts as a local source of momentum field on the right-hand-side of Eq. (2). Since its spatial integral has no reason to be wall independent, there is no reason for there to be an equation of state. In this paper, we show how to break down the active force field into equation-of-state-breaking and equation-of-state-nonbreaking terms, what aspect of the particle

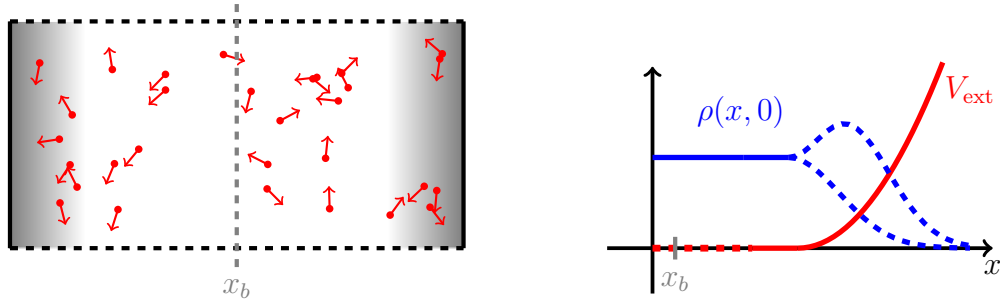


Figure 1. We consider a simple setting with vertical, flat, walls confining the particles along the \hat{x} direction while periodic boundary conditions are used along the \hat{y} direction. Active particles are unaffected by the interactions with the walls in the bulk of the system (white background). In the gray region, active particles experience a repulsive potential from the wall, which makes their density vanish at the wall boundary. On the right, two sketches of the density profiles are shown, with or without accumulation of active particles depending on the details of the potential and of the active dynamics. x_b refers to any position deep in the bulk of the system, far away from the walls.

dynamics gives rise to each, and how to interpret them. In section 1 we first consider the case of non-interacting particles. We show how torques exerted by the walls on the particles generically result in net steady-state sources or sinks of momentum localized close to the confining walls (sections 1.3 and 1.4). These momentum-non-conserving terms are wall-dependent and lead to a lack of an equation of state. Conversely, in the absence of such terms in the steady state, we introduce an effective momentum which includes a novel *active impulse* term, defined as the mean momentum a particle will receive on average from the substrate in the future (section 1.5), and related to the well-known swim pressure (section 1.6). This effective momentum satisfies a conservation law in the steady state, which restores the equation of state for the pressure of Refs. [9, 11] (section 1.7). In section 2 we generalize this discussion to the case of interacting particles and show how the same reasoning allows one to understand the emergence of an equation of state for pairwise forces and its absence for quorum-sensing interactions. We then discuss these results in the context of Motility-Induced Phase Separation (MIPS) [29] in section 3.

1. Noninteracting active particles

We first consider non-interacting active particles confined between two flat walls (see Fig. 1). For the sake of concreteness, we first derive our results in the case of an underdamped active Brownian particle model, described in section 1.1, before generalizing to a much wider class of models in Appendix A.

1.1. The Model

We consider active particles evolving in two spatial dimensions. Particle i , located at \mathbf{r}_i , evolves according to the dynamics:

$$\begin{aligned} \dot{\mathbf{r}}_i &= \mathbf{v}_i \\ m\dot{\mathbf{v}}_i &= -\tilde{\gamma}\mathbf{v}_i + f_i\mathbf{u}(\theta_i) - \nabla_{\mathbf{r}_i}V_{\text{ext}}(\mathbf{r}_i) + \sqrt{2\tilde{\gamma}^2D_t}\boldsymbol{\eta}_i . \end{aligned} \quad (4)$$

Here $\tilde{\gamma}$ is the friction coefficient, or inverse mobility, of the active particles, f_i their propulsive forces, V_{ext} is the potential exerted by the confining walls, and $\boldsymbol{\eta}_i$'s are Gaussian white noises satisfying $\langle \eta_i^\alpha(t) \rangle = 0$ and $\langle \eta_i^\alpha(t)\eta_j^\beta(t') \rangle = \delta_{i,j}\delta_{\alpha,\beta}\delta(t-t')$. Angular brackets denote an average over noise realizations. $\mathbf{u}(\theta_i)$ is a unit vector along the orientation θ_i of particle i . It evolves according to the overdamped dynamics

$$\dot{\theta}_i = \Gamma_i(\mathbf{r}_i, \theta_i) + \sqrt{2D_r}\zeta_i \quad (5)$$

where $\Gamma_i(\mathbf{r}_i, \theta_i)$ is the torque exerted on the particle by the wall scaled by the rotational mobility, and ζ_i is a Gaussian white noise with $\langle \zeta_i(t) \rangle = 0$ and $\langle \zeta_i(t)\zeta_j(t') \rangle = \delta_{i,j}\delta(t-t')$. Note that we consider underdamped dynamics, i.e. we retain the translational inertia of the particles, instead of the standard overdamped dynamics that we studied previously [13]

$$\mathbf{v}_i = \frac{1}{\tilde{\gamma}}f_i\mathbf{u}(\theta_i) - \frac{1}{\tilde{\gamma}}\nabla_{\mathbf{r}_i}V_{\text{ext}}(\mathbf{r}_i) + \sqrt{2D_t}\boldsymbol{\eta}_i . \quad (6)$$

A system of N such particles can always be characterized by its exact microscopic number density and momentum density fields

$$\hat{\rho}(\mathbf{r}) = \sum_{i=1}^N \delta(\mathbf{r} - \mathbf{r}_i) \quad \hat{\mathbf{p}}(\mathbf{r}) = \sum_{i=1}^N m\mathbf{v}_i\delta(\mathbf{r} - \mathbf{r}_i) , \quad (7)$$

These fields are fluctuating quantities whose averages with respect to noise realizations and initial conditions are defined by

$$\mathbf{p}(\mathbf{r}) = \langle \hat{\mathbf{p}}(\mathbf{r}) \rangle \quad \rho(\mathbf{r}) = \langle \hat{\rho}(\mathbf{r}) \rangle . \quad (8)$$

1.2. Momentum and Pressure

To proceed, we consider the dynamics of the momentum and density fields. The density field evolves according to

$$\partial_t \hat{\rho}(\mathbf{r}) = \sum_i \dot{\mathbf{r}}_i \cdot \nabla_{\mathbf{r}_i} \delta(\mathbf{r} - \mathbf{r}_i) = -\frac{1}{m} \nabla \cdot \hat{\mathbf{p}}(\mathbf{r}). \quad (9)$$

Here the subscript \mathbf{r}_i signals that the first gradient acts on the coordinates of particles i whereas the absence of a subscript in the last divergence signals that it acts on the position \mathbf{r} where the density is measured. This notation is used throughout the paper. Similarly, the dynamics of the momentum density field read

$$\begin{aligned} \partial_t \hat{\mathbf{p}} &= \sum_i \left(-\tilde{\gamma} \mathbf{v}_i - \nabla_{\mathbf{r}_i} V_{\text{ext}} + f_i \mathbf{u}(\theta_i) + \sqrt{2\tilde{\gamma}^2 D_t \eta_i} \right) \delta(\mathbf{r} - \mathbf{r}_i) + \sum_i m \mathbf{v}_i (\mathbf{v}_i \cdot \nabla_{\mathbf{r}_i}) \delta(\mathbf{r} - \mathbf{r}_i) \\ &= -\gamma \hat{\mathbf{p}} - \hat{\rho} \nabla V_{\text{ext}} + \sum_i f_i \mathbf{u}(\theta_i) \delta(\mathbf{r} - \mathbf{r}_i) + \sqrt{2\tilde{\gamma}^2 D_t \hat{\rho}} \mathbf{\Lambda} - \nabla \cdot [\mathcal{J}]. \end{aligned} \quad (10)$$

Here $\gamma \equiv \tilde{\gamma}/m$, and the tensor \mathcal{J} is defined by

$$\mathcal{J} \equiv \sum_i m \mathbf{v}_i \mathbf{v}_i \delta(\mathbf{r} - \mathbf{r}_i) \quad (11)$$

where $\mathbf{v}_i \mathbf{v}_i$ implies a tensor product[§]. The (i, j) component of the tensor \mathcal{J} is the flux along \hat{i} of momentum along \hat{j} . In addition, we have defined the Gaussian white noise $\sqrt{2\tilde{\gamma}^2 D_t \hat{\rho}} \mathbf{\Lambda} \equiv \sum_i \sqrt{2\tilde{\gamma}^2 D_t \eta_i} \boldsymbol{\eta}_i \delta(\mathbf{r} - \mathbf{r}_i)$ which can be verified to obey $\langle \Lambda_\alpha(\mathbf{r}, t) \Lambda_\beta(\mathbf{r}', t') \rangle = \delta_{\alpha\beta} \delta(\mathbf{r} - \mathbf{r}') \delta(t - t')$. Eq. (10) lists the various contributions leading to momentum density changes in \mathbf{r} : (i) loss of momentum due to dissipation, $-\gamma \hat{\mathbf{p}}$; (ii) forces due to the walls, $-\hat{\rho} \nabla V_{\text{ext}}$; (iii) active forces propelling the particles, $\sum_i f_i \mathbf{u}(\theta_i) \delta(\mathbf{r} - \mathbf{r}_i)$; (iv) fluctuations, $\sqrt{2\tilde{\gamma}^2 D_t \hat{\rho}} \mathbf{\Lambda}$; (v) advection of momentum as particles arrive in and depart from \mathbf{r} , $-\nabla \cdot [\mathcal{J}]$.

At steady state, in the confining potential shown in Fig. 1, Eq. (9) implies that $\mathbf{p}(\mathbf{r})=0$. Since the system is invariant under translations along \hat{y} we integrate Eq. (10) along the y coordinate and define $\rho(x) = \int_0^1 dy \rho(x, y)$. Here, to keep the notation simple, we set the extent of the system in the y direction to be unity and we silently omit the (lack of) dependence on y of the observables. This gives

$$0 = -\rho(x) \partial_x V_{\text{ext}}(x) + \left\langle \sum_i f_i \cos \theta_i \delta(x - x_i) \right\rangle - \partial_x [\langle \mathcal{J}^{xx}(x) \rangle] \quad (12)$$

[§] Note that $\langle \mathcal{J} \rangle$ is non-zero even in steady-state due to the trivial correlations between velocities and momenta.

where $\mathcal{J}^{xx} = \sum_i \delta(x - x_i) m (v_i^x)^2$. Eq. (12) states that the momentum flux is enhanced or suppressed as it travels through the system by either the wall force or the active forces.

The mechanical pressure exerted on the wall is then given by integrating Eq. (12) from a point x_b deep in the bulk of the system to $x = +\infty$

$$P \equiv \int_{x_b}^{\infty} dx \rho \nabla_x V_{\text{ext}} = \langle \mathcal{J}^{xx}(x_b) \rangle + \int_{x_b}^{\infty} \langle \sum_i f_i \cos \theta_i \delta(x - x_i) \rangle dx . \quad (13)$$

The total change of the momentum flux from its bulk value $\langle \mathcal{J}^{xx} \rangle$ to zero beyond the wall is the result of the total force exerted by the wall and of the total active force exerted in the $x > x_b$ region. Alternatively, Eq. (13) means that the pressure is equal to the momentum flux entering the $x > x_b$ region plus the total active force exerted in this region. Note that, since $\nabla_x V_{\text{ext}}$ vanishes in the bulk, P , as defined in (13), does not depend on the choice of x_b .

To have an EOS, the right-hand side of equation (13) has to solely depend on bulk quantities. This is clearly the case for $\langle \mathcal{J}^{xx}(x_b) \rangle$ which originates from the divergence of the momentum flux. On the contrary, the total active force exerted in the $x > x_b$ region has no reason to depend only on bulk properties. While in the bulk the isotropy of the steady-state implies that $\langle \sum_i f_i \cos \theta_i \delta(x - x_i) \rangle$ is zero, it is well known that near the wall a non-trivial orientational order develops which depends explicitly on the potential shape V_{ext} . It is thus natural to expect that the mean active force should generically give a wall-dependent contribution to the pressure, hence leading to a lack of equation of state. Note that neither the damping force $-\gamma \hat{p}$ nor the Langevin force $\sqrt{2\tilde{\gamma}^2 D_t \hat{\rho}} \mathbf{\Lambda}$ conserve momentum either. However, they average to zero in steady state and therefore do not affect the pressure directly.

Expectedly, setting $f_i = 0$ in our model gives back the equilibrium dynamics of underdamped colloidal particles. Eq. (13) then expresses the mechanical pressure in terms of a purely bulk quantity, $\langle \mathcal{J}^{xx}(x_b) \rangle$; this fleshes out the argument presented in the introduction after Eq. (3) and shows such equilibrium systems to admit an EOS.

We next illustrate how the active force influences the pressure for the system described by Eqs. (4) and (5).

1.3. The breakdown of the EOS: momentum sources and sinks

Using Itô calculus, the dynamics of the mean active force density is given by

$$\begin{aligned} \partial_t \langle \sum_i f_i \cos \theta_i \delta(x - x_i) \rangle &= - \langle \sum_i f_i \Gamma_i \sin \theta_i \delta(x - x_i) \rangle - D_r \langle \sum_i f_i \cos \theta_i \delta(x - x_i) \rangle \\ &\quad - \partial_x [\langle \sum_i v_i^x f_i \cos \theta_i \delta(x - x_i) \rangle] \end{aligned} \quad (14)$$

which in the steady state, gives the balance equation

$$\langle \sum_i f_i \cos \theta_i \delta(x - x_i) \rangle = - \langle \sum_i \frac{f_i}{D_r} \Gamma_i \sin \theta_i \delta(x - x_i) \rangle - \partial_x [\langle \sum_i \frac{v_i^x}{D_r} f_i \cos \theta_i \delta(x - x_i) \rangle]. \quad (15)$$

This states that the local active force is the sum of a torque-dependent term and a torque-independent one, the latter being the derivative of a *local* quantity. This local quantity is responsible for the advection of active forces and we discuss in details its physics in section 1.5.

The force balance equation (12) now becomes

$$\rho(x) \partial_x V_{\text{ext}}(x) = - \sum_i \langle \frac{f_i}{D_r} \Gamma_i \sin \theta_i \delta(x - x_i) \rangle - \partial_x \left[\sum_i \langle \frac{v_i^x}{D_r} f_i \cos \theta_i \delta(x - x_i) \rangle + \langle \mathcal{J}^{xx}(x) \rangle \right]. \quad (16)$$

Eq. (10) identified the active forces as momentum sources, in agreement with the idea that each particle is receiving momentum from the substrate. Eqs. (15) and (16) show that the steady-state mean active force density can be split between a “momentum-conserving” part, *i.e.* the divergence of a local tensor, and a torque-dependent “non-conserving” term, *i.e.* a steady-state momentum source or sink. Note that this “effective momentum conservation” is restricted to the steady-state and we discuss it in more detail in section 1.5 and 1.7. For now, we focus on the pressure, which can be written as

$$P = \langle \mathcal{J}^{xx}(x_b) \rangle + \sum_i \langle \frac{v_i^x}{D_r} f_i \cos \theta_i \delta(x_b - x_i) \rangle - \int_{x_b}^{\infty} dx \langle \frac{f_i}{D_r} \Gamma_i \sin \theta_i \delta(x - x_i) \rangle, \quad (17)$$

where x_b is a point deep in the bulk of the system. The first two terms depend only on bulk properties of the fluid, while the latter is responsible for a wall-dependent contribution to the pressure. The breakdown of the equation of state thus arises from wall-dependent active sources. Eq. (15) shows that these sources can be measured by removing the contribution of the advective active-force term from the total contribution of the active force. Namely, by looking at

$$\Delta f_{\text{act}}(x) \equiv \langle \sum_i f_i \cos \theta_i \delta(x - x_i) \rangle + \partial_x \langle \frac{v_i^x}{D_r} f_i \cos \theta_i \delta(x - x_i) \rangle. \quad (18)$$

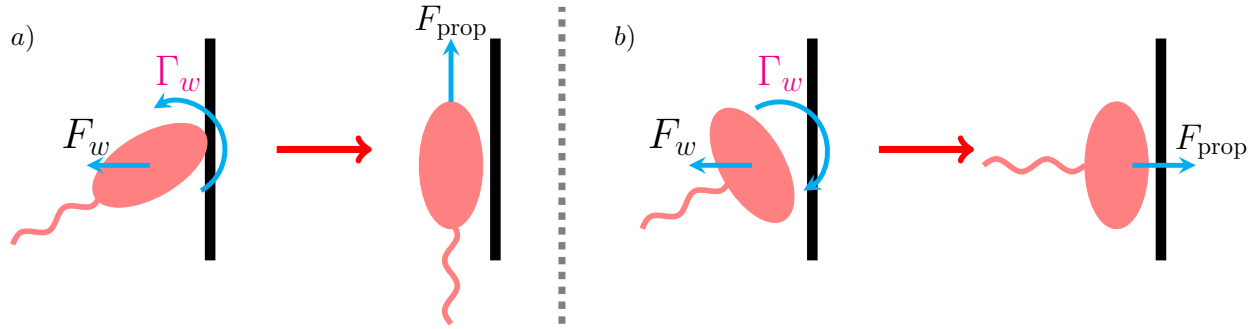


Figure 2. Impact of wall torques on the active contribution to the mechanical pressure. *a)* Torques that make active particles align their propulsive forces along the wall diminish their contributions to the overall force exerted on the wall. *b)* On the contrary, torques making the active particles face the wall increase the contributions of the active forces to the mechanical pressure.

The relation is, as will become clearer later, more general and can be used to identify the presence of steady-state momentum sources for any model of active Brownian particles. For the model we consider here, in the presence of wall torques, the non-conserving terms are given by

$$\Delta f_{\text{act}}(x) = - \sum_i \left\langle \frac{f_i}{D_r} \Gamma_i \sin \theta_i \delta(x - x_i) \right\rangle. \quad (19)$$

Figure 2 offers a more intuitive picture of the way wall torques affect the pressure. The active pressure comes from the transmission of the momentum received by the particles from the substrate to the walls. If torques are such that particles align and move along the wall, the momentum they transmit to the wall is reduced (compared to say, torque-less particles). Conversely, if torques force the particle to face the walls, the transmission of active force to the wall is enhanced.

All in all, Eq. (13) shows the pressure to be related to the mean active forces experienced by the particles. Even though each of these forces injects momentum into the system, Eq. (15) shows the mean active force in steady state to be composed of two contributions: a torque-dependent source, measured in Eq. (18), and a momentum-conserving one. Before focusing on the torque-free case (section 1.5) and showing how to interpret those results in terms of an effective momentum conservation (section 1.7), let us numerically illustrate our results so far.

1.4. Numerical measurement of sources and sinks

We consider self-propelled particles evolving under the dynamics (4) and (5), confined by harmonic walls modelled by the repulsive potentials

$$V^R(x) = \lambda_R \frac{(x - x_w)^2}{2} \Theta(x - x_w) \quad \text{and} \quad V^L(x) = \lambda_L \frac{(x + x_w)^2}{2} \Theta(-x - x_w) \quad (20)$$

for right and left walls, respectively. Here $\Theta(x)$ denotes a Heaviside function. The particles are modeled as ellipses of principle axes a and b , with the self-propulsion being along the a axis. We consider the limit in which the particles are ‘point-like’ (*i.e.* much smaller than their penetration length into the wall potential) so that the torques they experience from the walls can be computed explicitly as

$$\Gamma^R(x, \theta) = \lambda_R \kappa \Theta(x - x_w) \sin 2\theta \quad \text{and} \quad \Gamma^L(x, \theta) = \lambda_L \kappa \Theta(-x - x_w) \sin 2\theta \quad (21)$$

where $\kappa = \mu_r(a^2 - b^2)$ measures the anisotropy of the particles and μ_r is a rotational mobility [13]. In practice, we took $x_b = 0$ in all our simulations (See Eq. 13), making sure that the system size was large enough that a moderate change in x_b did not change our results.

The three contributions to the pressure P defined in Eq. (17) are shown in the left panel of Fig. 3 for walls with $\lambda_R = \lambda_L = \lambda$. The figure shows that only the torque-dependent contributions depend on the wall stiffness λ . The corresponding wall-dependent sources and sinks $\Delta f_{\text{act}}(x)$ are shown in the right panel of Fig. 3 for three stiffnesses.

An important consequence of those sources appears when the particles are confined by left and right walls with different stiffness $\lambda_R \neq \lambda_L$. Integrating Eq. (12) over the whole space shows that the difference between the pressures measured on the left and right walls is equal to the total active force in the system:

$$P_R - P_L \equiv \int_{-\infty}^{\infty} \sum_i \langle f_i \cos \theta_i \delta(x - x_i) \rangle dx \quad (22)$$

This shows that when the system is confined between two walls with different stiffnesses there may be a net force acting on the boundaries. Eq. (16) then shows this total active force to be given by the torque-dependent sources

$$P_R - P_L = \int_{-\infty}^{\infty} \Delta f_{\text{act}}(x) dx = - \int_{-\infty}^{\infty} \sum_i \langle \frac{f_i}{D_r} \Gamma_i \sin \theta_i \delta(x - x_i) \rangle dx, \quad (23)$$

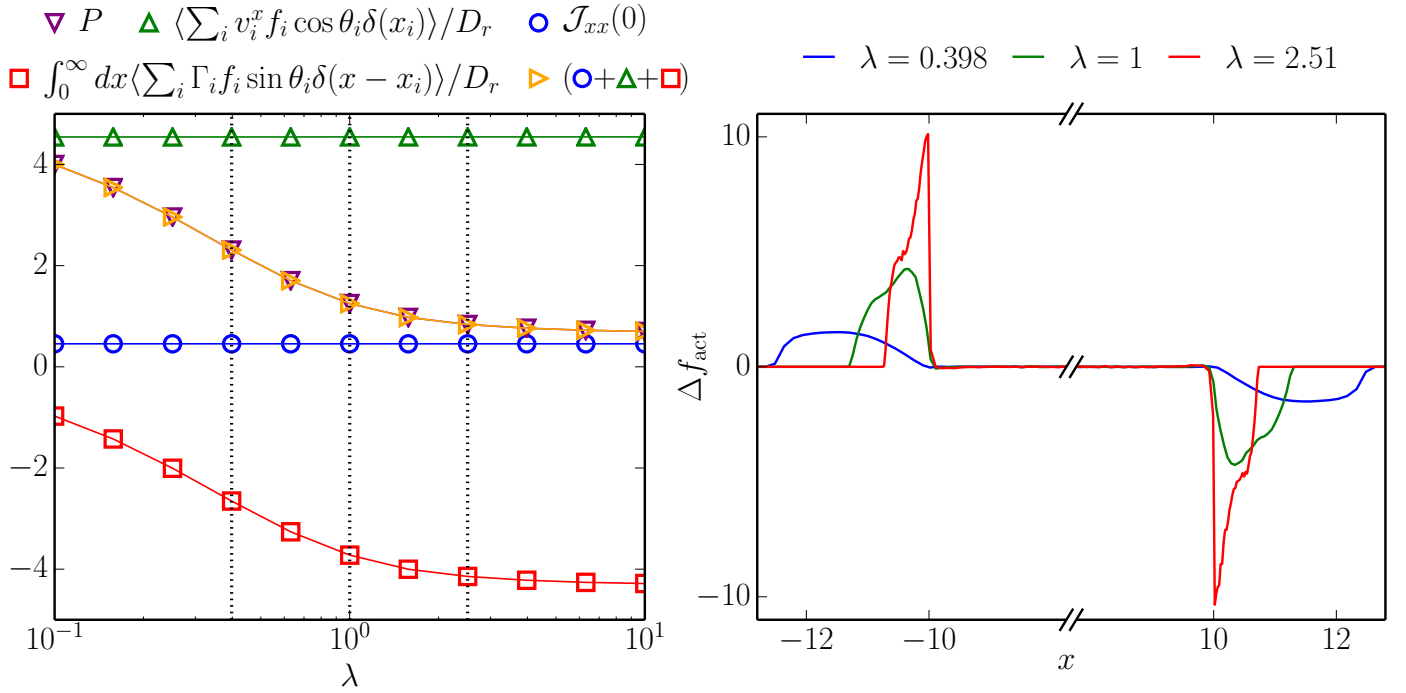


Figure 3. Brownian dynamics simulations of self-propelled ellipses with bulk density $\rho_0 = 1$ confined between harmonic walls located at $x = \pm x_w$ for $x_w = 10$, $f_i = 1$, $D_r = 0.1$, $D_t = 0$, $\tilde{\gamma} = 1$, $m = 1$, $\kappa = 1$. **Left:** Wall pressure and its various contributions as a function of the wall stiffness λ . The pressure measured from the definition Eq. (13) (purple triangles) matches the one obtained from Eq. (17) (yellow triangles). Of the three contributions to the latter (green triangles, blue circles, red squares), only the one due to wall torques (red squares) depends on the wall stiffness, leading to a breakdown of the EOS. **Right:** Spatial profiles of the wall-dependent momentum sources defined by Eq. (18) for three different values of λ showing its localization in the vicinity of the walls. The three values of λ appear as vertical dotted lines in the left panel.

as illustrated in Fig. 4. This validates our interpretation of Δf_{act} as the net steady-state sources and sinks of momentum. So far, we have shown that the existence of an EOS depends on the fact that the dynamics of the momentum density field takes the form of a conservation equation in steady-state. We now discuss in more detail the underlying physical interpretation.

1.5. Torque-free active gas: active impuse and the emergence of an equation of state

We now consider torque-free active particles and discuss why an equation of state is recovered in this case. In particular, we show this to be a property shared by all systems where the dynamics of the active force $f_i \mathbf{u}_i$ are decoupled from other degrees of freedom and lead to $\langle f_i \mathbf{u}_i \rangle = 0$ in steady-state. In the main text, we consider the case of torque-free rotational diffusion while a more general case is addressed in Appendix A.

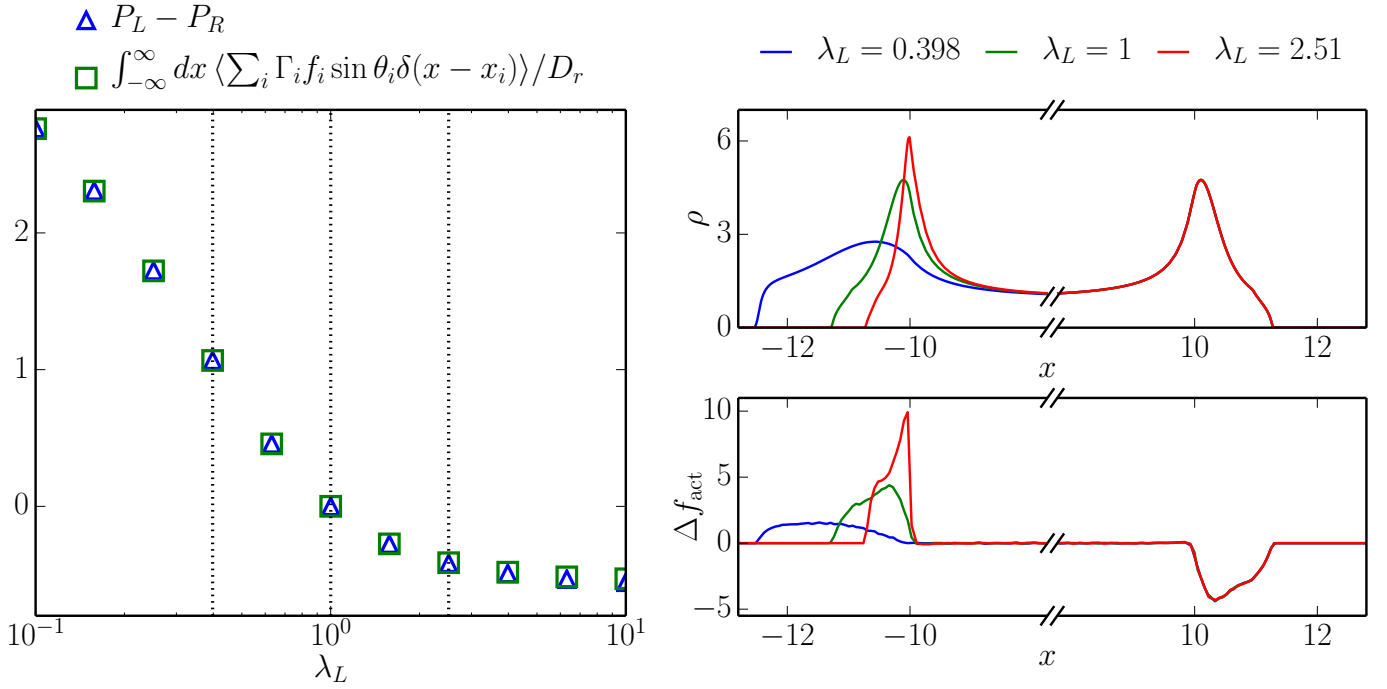


Figure 4. Brownian dynamics simulations of self-propelled ellipses confined between harmonic walls with stiffnesses $\lambda_R = 1$ on the right and λ_L on the left. All other parameters are identical to Fig. 3. **Left:** Pressure difference between the two walls as a function of λ_L . Different stiffnesses ($\lambda_L \neq \lambda_R$) lead to a difference of pressure between the two walls (blue triangles). It is fully accounted for by the torque-dependent contribution to the total active force (green squares). **Right:** Spatial profile of the density (top) and the wall-dependent momentum source defined by Eq. (18) (bottom) for three different values of λ_L , indicated by vertical dotted lines in the left panel.

The contribution of the activity to the pressure stems from the momentum transferred to the particles through the active forces. This can be quantified by the “active impulse” which measures the momentum the active particle will receive on average from its active force in the future. For the case of pure, torque-free rotational diffusion, this can be readily computed as

$$\Delta \mathbf{p}_i^a(t) \equiv \int_t^{\infty} \overline{f_i \mathbf{u}[\theta_i(\mathbf{s})]} ds = \frac{f_i}{D_r} \mathbf{u}[\theta_i(t)] \quad (24)$$

where the overline denotes an average with respect to histories of the system in the time interval $[t, +\infty)$ for a given value of $\theta_i(t)$. In (24), the active impulse simply depends on the initial angle $\theta_i(t)$ because the dynamics of the active force $f \mathbf{u}_i$ is independent of all other degrees of freedom. For a more general discussion, we refer the reader to Appendix A.

By construction, the dynamics of the active impulse obey

$$\partial_t \Delta \mathbf{p}_i^a(t) = -f_i \mathbf{u}[\theta_i(t)] . \quad (25)$$

In turn, the dynamics of the mean active-impulse field $\langle \Delta \mathbf{p}^a(x) \rangle = \langle \sum_i \Delta \mathbf{p}_i^a \delta(\mathbf{r} - \mathbf{r}_i) \rangle$ is given by:

$$\partial_t \langle \Delta \mathbf{p}^a(x) \rangle = - \langle \sum_i f_i \mathbf{u}[\theta_i(s)] \delta(\mathbf{r} - \mathbf{r}_i) \rangle - \nabla \cdot \langle \sum_i \mathbf{v}_i \Delta \mathbf{p}_i^a \delta(\mathbf{r} - \mathbf{r}_i) \rangle \quad (26)$$

where the divergence ∇ is contracted with the velocities \mathbf{v}_i . This gives in the steady state

$$\langle \sum_i f_i \mathbf{u}[\theta_i(s)] \delta(\mathbf{r} - \mathbf{r}_i) \rangle = - \nabla \cdot \langle \sum_i \mathbf{v}_i \Delta \mathbf{p}_i^a \delta(\mathbf{r} - \mathbf{r}_i) \rangle \quad (27)$$

$$= - \nabla \cdot \langle \sum_i \mathbf{v}_i \frac{f_i}{D_r} \mathbf{u}(\theta_i) \delta(\mathbf{r} - \mathbf{r}_i) \rangle. \quad (28)$$

Despite each active force injecting momentum into the system, Eq. (28) shows that their average contribution in the steady state takes a momentum-conserving form, namely the mean local active force can be written as the divergence of a local tensor. This can be understood as follows. In any volume element, the mean active force decays to zero because of rotational diffusion. A non-vanishing mean local active force can thus only be sustained by incoming fluxes of particles which carry their active force with them. This is quantified by the tensor measuring the flux of active impulse

$$\mathcal{G} \equiv \sum_i \mathbf{v}_i \frac{f_i}{D_r} \mathbf{u}(\theta_i) \delta(\mathbf{r} - \mathbf{r}_i). \quad (29)$$

$\langle \mathcal{G}(\mathbf{r}) \rangle$ is non-zero because of the correlations between the velocities of the particles and their active forces.

With the above results, expression (13) for the pressure can now be written as

$$P = \langle \mathcal{J}^{xx}(x_b) \rangle + \int_{x_b}^{\infty} \langle \sum_i f_i \cos \theta_i \delta(x - x_i) \rangle dx = \langle \mathcal{J}^{xx}(x_b) \rangle + \langle \mathcal{G}^{xx}(x_b) \rangle. \quad (30)$$

This expression clearly depends solely on bulk quantities and constitutes the EOS of the mechanical pressure in the absence of torques. The correlators appearing in (30) can be computed using Itô-calculus.

Let us first compute

$$\begin{aligned} \partial_t \langle \sum_i f_i \cos \theta_i v_i^x \delta(x - x_i) \rangle &= - \frac{\tilde{\gamma}}{m} \langle \sum_i f_i \cos \theta_i v_i^x \delta(x - x_i) \rangle + \langle \sum_i \frac{1}{m} f_i^2 \cos^2 \theta_i \delta(x - x_i) \rangle \\ &\quad - D_r \langle \sum_i f_i \cos \theta_i v_i^x \delta(x - x_i) \rangle - \partial_x \langle \sum_i f_i \cos \theta_i (v_i^x)^2 \delta(x - x_i) \rangle \end{aligned}$$

Since all particles have the same propulsive force $f_i = f$, one finds in a homogeneous, isotropic bulk of density ρ_0 , where $\langle \cos^2 \theta_i \rangle = 1/2$, that

$$(D_r + \frac{\tilde{\gamma}}{m}) \langle \sum_i f \cos \theta_i v_i^x \delta(x - x_i) \rangle = \frac{\rho_0 f^2}{2m} \quad (31)$$

We then consider

$$\begin{aligned} \partial_t \left\langle \sum_i \frac{m(v_i^x)^2}{2} \delta(x - x_i) \right\rangle &= -\tilde{\gamma} \left\langle \sum_i (v_i^x)^2 \delta(x - x_i) \right\rangle + \left\langle \sum_i f_i v_i^x \cos \theta_i \delta(x - x_i) \right\rangle \\ &\quad + \frac{\tilde{\gamma}^2 D_t}{m} \sum_i \delta(x - x_i) - \partial_x \left\langle \sum_i \frac{m(v_i^x)^3}{2} \delta(x - x_i) \right\rangle \end{aligned}$$

which yields in the steady-state of the homogeneous bulk

$$\left\langle \sum_i (v_i^x)^2 \delta(x - x_i) \right\rangle = \frac{\tilde{\gamma} \rho_0 D_t}{m} + \frac{1}{\tilde{\gamma}} \left\langle \sum_i f_i v_i^x \cos \theta_i \delta(x - x_i) \right\rangle \quad (32)$$

Using both the definitions (11) and (29) and the results (31) and (32), one then finds

$$\langle \mathcal{G}^{xx}(x_b) \rangle = \rho_0 \frac{f^2}{2D_r(mD_r + \tilde{\gamma})} \quad \text{and} \quad \langle \mathcal{J}^{xx}(x_b) \rangle = \rho_0 \left(\tilde{\gamma} D_t + \frac{mf^2}{2\tilde{\gamma}(\tilde{\gamma} + mD_r)} \right) \quad (33)$$

leading to the previously known expression for the pressure of a torque-less dry active system

$$P = \rho_0 \left(\tilde{\gamma} D_t + \frac{f^2}{2D_r \tilde{\gamma}} \right) \quad (34)$$

Despite $\langle \mathcal{G}^{xx}(x_b) \rangle$ and $\langle \mathcal{J}^{xx}(x_b) \rangle$ both depending on the mass of the particles, Eq. (34) shows the overall pressure to be independant of the mass. (This is illustrated in Fig. 5 for the system introduced in section 1.4.) Overdamped and underdamped dynamics thus have the same pressure.

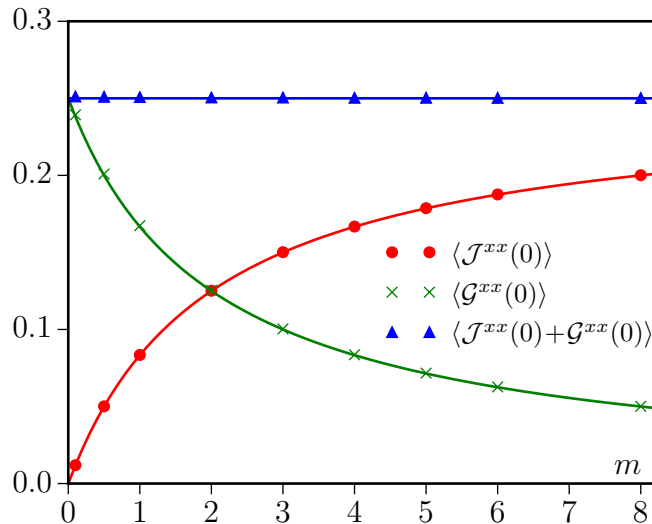


Figure 5. Brownian dynamics simulation of self-propelled disks with $\tilde{\gamma} = 2$, $f_i = 1$, $D_r = 1$, $\rho_0 = 1$, $\lambda = 1$, $D_t = 0$. The mean momentum and active impulse fluxes $\langle \mathcal{J}^{xx}(0) \rangle$ and $\langle \mathcal{G}^{xx}(0) \rangle$ depend on the particles mass m but their sum, which yields the pressure, remains constant. Solid lines correspond to the theoretical predictions (33) and (34) while symbols stem from numerical measurements.

It is illuminating to restate the above discussion for the appearance of an equation of state from both a global and a local picture.

Global picture of the EOS. Eq. (30) relies on the fact that the total active force exerted in the $x > x_b$ region is equal to the flux of free active impulse through the $x = x_b$ plane. In the absence of any bias in the dynamics of the active force, an active particle experiences on average a vanishing active force in steady-state. The presence of a wall at the right end of the system may alter its trajectory, but not the statistics of its active force. The only contribution that makes the mean active force non-zero in the $x > x_b$ region is thus that particles entering (leaving) this region typically have a positive (negative) component of their propulsive force along x . The magnitude of the mean active force in this region is thus directly measured by the flux of active impulse through the $x = x_b$ interface.

Local picture of the EOS. Let us now discuss what happens in the vicinity of a confining wall at the right end of the system. In the bulk, the flux of momentum $\langle \mathcal{J}^{xx} \rangle$ and of active impulse $\langle \mathcal{G}^{xx} \rangle$ are uniform. In the presence of an external force, Eqs. (12) and (28-29) lead to

$$\rho \partial_x V_{\text{ext}} = -\partial_x [\langle \mathcal{J}^{xx} + \mathcal{G}^{xx} \rangle]. \quad (35)$$

This states that the force (density) exerted by the wall generates a decay of the incoming fluxes of momentum and active impulse. This can be easily understood: for a passive system, the wall stops the particles by applying forces that decrease their momentum. The overall drop of the momentum flux from its bulk value to zero is then nothing but the pressure. For active particles, in addition to decreasing the momentum of the active particles, the wall has to compensate the momentum they gain due to the active force, i.e. it has to “consume” the active impulse of the particles.

Equation (35) shows the wall force to generate a non-zero divergence of the momentum and active impulse fluxes. In turn, the latter yield a layer of active force density close to the wall, according to Eqs. (28-29). The shape of this layer will typically depend on the confining potential, but since the integrated action of the wall potential is to bring the incoming fluxes from their bulk value to zero, the total active force, and hence its contribution to pressure, will not depend on the wall potential. This is illustrated in Fig. (6) for the system described in section 1.4.

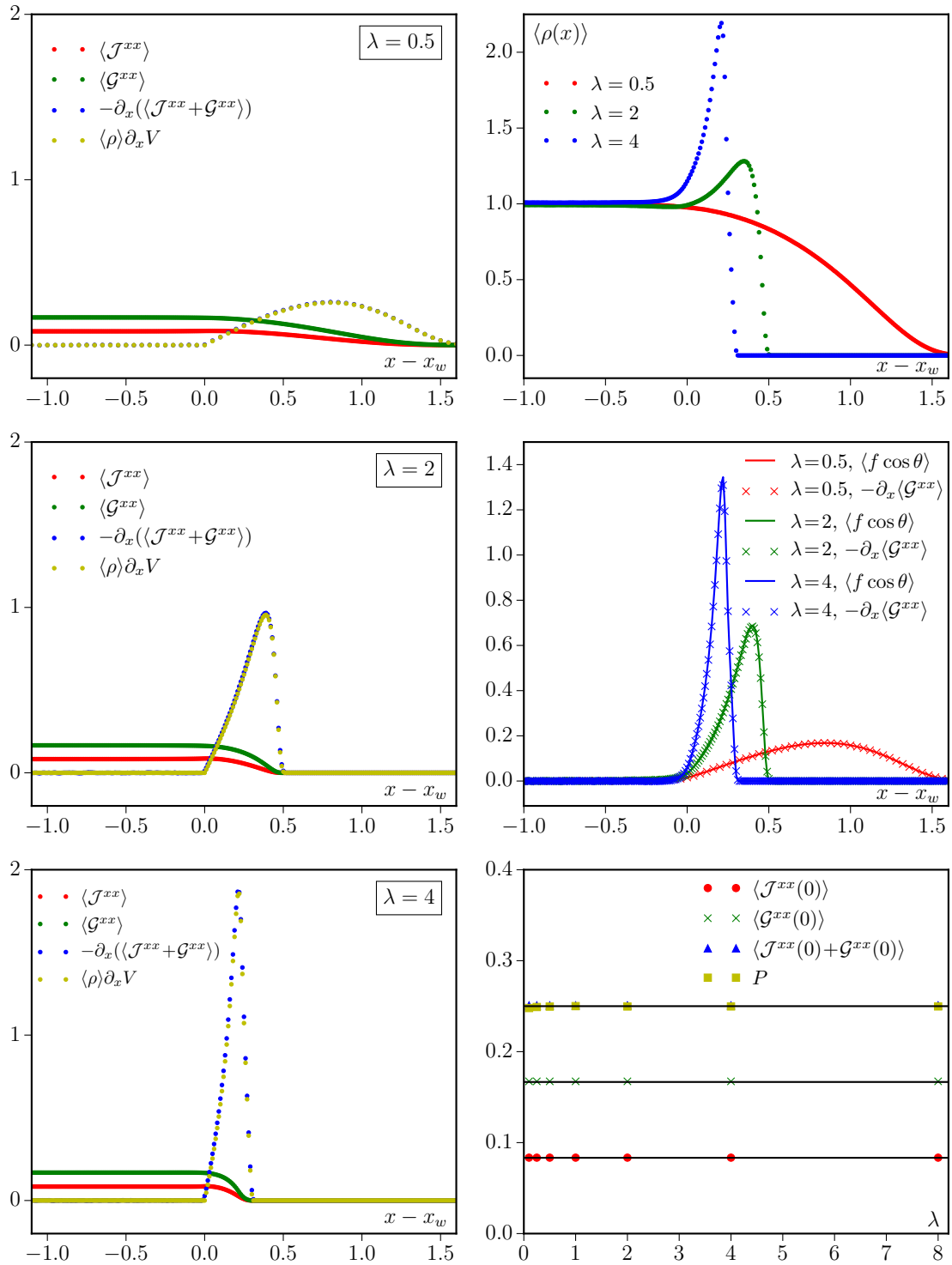


Figure 6. Brownian dynamics simulations of self-propelled disks confined by walls of different stiffness ($\lambda = 0.5, 2, 4$) for $f_i = 1$, $D_r = 1$, $D_t = 0$, $\tilde{\gamma} = 2$, $m = 1$, $\rho_0 = 1$. **Left:** Momentum (red) and active impulse (green) fluxes. The wall force (yellow) is exactly balanced by the divergence of the incoming momentum and active impulse fluxes. **Top right:** Number density showing wall-dependent boundary layers. **Middle right:** The average active force is given by (minus) the divergence of the incoming active impulse flux. **Bottom right:** Numerical measurements of the pressure, $\langle \mathcal{G}^{xx}(0) \rangle$, $\langle \mathcal{J}^{xx}(0) \rangle$ and their sum (symbols), compared with their theoretical predictions (solid lines) for varying wall stiffness.

1.6. Active impulse and swim pressure

Before we discuss in more detail the connection between the EOS and the effective conservation of momentum, we note that the flux of active impulse $\langle \mathcal{G} \rangle$ can be expressed in a slightly different manner.

To do so, we use

$$\partial_t \langle \mathbf{r}_i f_i \mathbf{u}(\theta_i) \rangle = \langle \mathbf{v}_i f_i \mathbf{u}(\theta_i) \rangle - D_r \langle \mathbf{r}_i f_i \mathbf{u}(\theta_i) \rangle, \quad (36)$$

Therefore, in the steady state one can express $\langle \mathcal{G} \rangle$ as

$$\langle \mathcal{G}(\mathbf{r}) \rangle = \langle \delta(\mathbf{r} - \mathbf{r}_i) \mathbf{r}_i f_i \mathbf{u}(\theta_i) \rangle. \quad (37)$$

This expression was introduced in [11] and termed the swim-pressure. It can also be found using an approach generalizing the virial theorem [19, 23] or following Irving and Kirkwood [9]. Note, however, that the discussion above makes it clear that this does not, in general, provide the expression for the pressure unless an effective momentum conservation within the active fluid is present in the steady state. Moreover, the equality between the active force and \mathcal{G} , whether its expressions (29) or (37), only holds in the steady state. Last, conservation laws are typically defined dynamically, whereas our derivation only holds in the steady-state, we now discuss a more precise definition of what we mean by effective momentum conservation in the steady-state.

1.7. Effective steady-state momentum conservation

Let us first consider the torque-free non-interacting active particles of section 1.5. In this case, the dynamics of the mean momentum density field can be obtained from Eq. (10)

$$\partial_t \mathbf{p} = -\gamma \mathbf{p} - \rho \nabla V_{\text{ext}} + \left\langle \sum_i f_i \mathbf{u}(\theta_i) \delta(\mathbf{r} - \mathbf{r}_i) \right\rangle - \nabla \cdot [\langle \mathcal{J} \rangle]. \quad (38)$$

There are three sources of momentum for the active particles in the steady state: the external wall, through $-\rho \nabla V_{\text{ext}}$, the friction with the substrate, through $-\gamma \mathbf{p}$, and the active forces. Using the definition of the active impulse (24) and its dynamics (26), the mean active force density can always be replaced by

$$\left\langle \sum_i f_i \mathbf{u}[\theta_i(s)] \delta(\mathbf{r} - \mathbf{r}_i) \right\rangle = -\partial_t \langle \Delta \mathbf{p}^a(x) \rangle - \nabla \cdot \left\langle \sum_i \mathbf{v}_i \Delta \mathbf{p}_i^a \delta(\mathbf{r} - \mathbf{r}_i) \right\rangle \quad (39)$$

so that the dynamics of the momentum field can be written as

$$\partial_t \mathbf{p} = -\gamma \mathbf{p} - \partial_t \langle \Delta \mathbf{p}^a(x) \rangle - \rho \nabla V_{\text{ext}} - \nabla \cdot [\langle \mathcal{J} + \mathcal{G} \rangle]. \quad (40)$$

In steady-state, the first two terms on the right-hand side vanish and the sole non-vanishing momentum source is the external wall. Outside steady-state, however, \mathbf{p} is not conserved even in the absence of external walls. Note that Eq. (40) can be rewritten as

$$\partial_t [\mathbf{p} + \langle \Delta \mathbf{p}^a(x) \rangle] = -\gamma \mathbf{p} - \rho \nabla V_{\text{ext}} - \nabla \cdot [\langle \mathcal{J} + \mathcal{G} \rangle]. \quad (41)$$

This equation states that, apart from the friction force and the external forces, the sum of the momentum of the particles \mathbf{p} and of their active impulse $\Delta \mathbf{p}^a$ is conserved. The latter acts as a momentum reservoir for the particles: when the active impulse varies, it is through a transfer of momentum to the active particles via the active forces. Since the friction term $-\gamma \mathbf{p}$ vanishes in steady-state, this is probably the cleanest way of expressing what we mean by effective steady-state conservation of momentum in this system.

The breakdown of the equation of state in the case with external torques can then be understood from two different viewpoints. First, one can keep the definition of the active impulse of a particle as an intrinsic property:

$$\Delta \mathbf{p}_i^a(t) \equiv \frac{f_i}{D_r} \mathbf{u}(\theta_i(t)) \quad (42)$$

which corresponds to the active impulse of a particle in the absence of any external wall (say, for periodic boundary conditions). In the presence of wall torques, Eq. (41) then becomes

$$\partial_t [\mathbf{p} + \langle \Delta \mathbf{p}^a(x) \rangle] = -\gamma \mathbf{p} - \rho \nabla V_{\text{ext}} - \int_{x_b}^{\infty} dx \langle \frac{f_i}{D_r} \Gamma_i \sin \theta_i \delta(x - x_i) \rangle - \nabla \cdot [\langle \mathcal{J} + \mathcal{G} \rangle]. \quad (43)$$

This highlights a new source of momentum for the particles stemming from wall torques.

An alternative view can be obtained if one keeps the definition of the active impulse as

$$\Delta \mathbf{p}_i^a(t) \equiv \int_t^{\infty} \overline{f_i \mathbf{u}[\theta_i(\mathbf{s})]} ds, \quad \text{whence} \quad \Delta \mathbf{p}_i^a(t) \neq \frac{f_i}{D_r} \mathbf{u}[\theta_i(t)]. \quad (44)$$

The last equality does not hold since encounters between a particle and the wall changes its orientation and hence its momentum and active impulse: the active impulse is then not a local quantity anymore. This can be understood by noting that the definition (44) is non-local in time. This translates into a

non-locality in space because of the motion of the particles during $[t, +\infty)$ and the active impulse of a particle in the bulk of the system depends on its fate upon future encounters with the walls. With this definition, one can then still relate the pressure to the fluxes of momentum and of active impulse through

$$P = \langle \mathcal{J}^{xx} + \mathcal{G}^{xx} \rangle \quad \text{with} \quad \mathcal{G} \equiv \sum_i \mathbf{v}_i \Delta \mathbf{p}_i^a \delta(\mathbf{r} - \mathbf{r}_i). \quad (45)$$

But \mathcal{G} is not given anymore by the local tensor (29) and becomes a *non-local* quantity, which depends on the wall stiffness so that (45) does not yield an equation of state anymore. Both interpretations are equally valid, but (42) makes the role of wall torques as momentum sources more explicit and this is the path we follow in this article.

Now that we have extensively discussed the case of non-interacting active particles, we show our results to extend to interacting active particles in section 2 and discuss their implications for phase-separating systems in section 3.

2. Interacting active particles

In what follows we now include interactions between particles and study their effect on the existence or absence of an equation of state. To do this, we consider torque-free particles and look at two models—quorum sensing interactions and pairwise interactions. In the overdamped limit, it is known that the first does not admit an equation of state while the latter does [13, 14]. As shown below this also holds for the underdamped model and is, as in the non-interacting case, directly related to the presence or absence of momentum sources and sinks in the steady state.

The equations of motion, allowing for both quorum sensing and pairwise interactions, are:

$$\begin{aligned} \dot{\mathbf{r}}_i &= \mathbf{v}_i \\ m\dot{\mathbf{v}}_i &= -\tilde{\gamma}\mathbf{v}_i + f_i(\{\mathbf{r}\})\mathbf{u}(\theta_i) + \mathbf{F}_i(\{\mathbf{r}\}) - \nabla_{\mathbf{r}_i} V_{ext} + \sqrt{2\tilde{\gamma}^2 D_t \eta_i} \\ \dot{\theta}_i &= \sqrt{2D_r \zeta_i}, \end{aligned} \quad (46)$$

where $\{\mathbf{r}\} = \{\mathbf{r}_1, \mathbf{r}_2, \dots\}$ is the collection of coordinates of all the particles. Note that we allow the magnitude of the active force $f_i(\{\mathbf{r}\})$ to depend on the locations of the other particles. In addition

we consider inter-particle forces $\mathbf{F}_i(\{\mathbf{r}\})$. All these interactions are assumed to be short ranged. It is a straightforward exercise to extend the model to include a dependence of the active force f_i and the force \mathbf{F}_i on the orientations of all the particles or to include interparticle aligning torques (see [13] for a discussion of this case in the overdamped limit). Since such angular dependences do not alter our conclusions qualitatively, we do not detail here the results concerning these cases.

As before, we consider the dynamics of the momentum density field, which is now given by

$$\partial_t \mathbf{p} = -\gamma \mathbf{p} - \rho \nabla V_{ext} + \sum_i \langle f_i(\{\mathbf{r}\}) \mathbf{u}(\theta_i) \delta(\mathbf{r} - \mathbf{r}_i) \rangle + \sum_i \langle \mathbf{F}_i(\{\mathbf{r}\}) \delta(\mathbf{r} - \mathbf{r}_i) \rangle - \nabla \cdot \langle \mathcal{J} \rangle \quad (47)$$

where we use the notations of the previous section. For the flat wall geometry of Fig. 1, one gets

$$P = \langle \mathcal{J}^{xx}(x_b) \rangle + \int_{x_b}^{\infty} \langle \sum_i f_i(\{\mathbf{r}\}) \cos \theta_i \delta(x - x_i) \rangle dx + \int_{x_b}^{\infty} \langle \sum_i F_i^x(\{\mathbf{r}\}) \delta(x - x_i) \rangle dx, \quad (48)$$

where F_i^x is the x -component of the force \mathbf{F}_i and we use the convention introduced before Eq. (12) so that an integration over the \hat{y} direction is carried out. To look for a possible effective momentum conservation which, much like in the non-interacting case, will lead to an equation of state, one needs to analyze the last two terms in Eq. (48). Note that, as before, we assume that the bulk steady-state is uniform.

In what follows it will be helpful to use the relation

$$\begin{aligned} \partial_t \langle f_i \cos \theta_i \delta(x - x_i) \rangle &= \sum_j \langle \mathbf{v}_j \cdot (\nabla_{\mathbf{r}_j} f_i) \cos \theta_i \delta(x - x_i) \rangle + \langle v_i^x f_i \cos \theta_i \partial_{x_i} \delta(x - x_i) \rangle \\ &\quad - D_r \langle f_i \cos \theta_i \delta(x - x_i) \rangle, \end{aligned} \quad (49)$$

which gives in the steady state

$$\langle f_i \cos \theta_i \delta(x - x_i) \rangle = \sum_j \langle \mathbf{v}_j \cdot (\nabla_{\mathbf{r}_j} \frac{f_i}{D_r}) \cos \theta_i \delta(x - x_i) \rangle - \partial_x \langle v_i^x \frac{f_i}{D_r} \cos \theta_i \delta(x - x_i) \rangle \quad (50)$$

$$= \sum_j \langle \mathbf{v}_j \cdot (\nabla_{\mathbf{r}_j} \frac{f_i}{D_r}) \cos \theta_i \delta(x - x_i) \rangle - \partial_x \langle \mathcal{G}^{xx} \rangle. \quad (51)$$

This shows that, due to the dependence of the self-propulsion force f_i on the \mathbf{r}_j 's, the density of active forces is not purely given by the divergence of the flux of the active impulse \mathcal{G} defined in (29). Together with Eq. (48), this suggests a potential breakdown of the equation of state. The measure of active

sources Δf_{act} , defined in Eq. (18), is now given by

$$\Delta f_{\text{act}}(x) = \left\langle \sum_i f_i \cos \theta_i \delta(x - x_i) \right\rangle + \partial_x \left\langle \frac{v_i^x}{D_r} f_i \cos \theta_i \delta(x - x_i) \right\rangle \quad (52)$$

$$= \sum_j \left\langle \mathbf{v}_j \cdot \left(\nabla_{\mathbf{r}_j} \frac{f_j}{D_r} \right) \cos \theta_j \delta(x - x_j) \right\rangle \quad (53)$$

Let us first treat the case of pure quorum sensing and discuss afterwards interparticle forces $\mathbf{F}_i(\{\mathbf{r}\})$.

2.1. Quorum sensing

In models of quorum sensing the active force of a particle is modulated according to the density of particles in a region around it. To make the discussion clearer we assume that $\mathbf{F}_i(\{\mathbf{r}\}) = 0$. Using Eq. (50) one finds that the pressure is given by

$$P = \langle \mathcal{J}^{xx}(x_b) \rangle + \langle \mathcal{G}^{xx}(x_b) \rangle + \int_{x_b}^{\infty} \left\langle \sum_j \mathbf{v}_j \cdot \left(\nabla_{\mathbf{r}_j} \frac{f_j}{D_r} \right) \cos \theta_j \delta(x - x_j) \right\rangle dx \quad (54)$$

$$= \langle \mathcal{J}^{xx}(x_b) \rangle + \langle \mathcal{G}^{xx}(x_b) \rangle + \int_{x_b}^{\infty} \Delta f_{\text{act}}(x) dx \quad (55)$$

where as before x_b is a point in the bulk of the system. The only term which may act as a momentum source/sink is the last one. At any position x_b in the bulk, the system is isotropic in the steady-state and

$$\Delta f_{\text{act}}(x_b) = \left\langle \sum_j \mathbf{v}_j \cdot \left(\nabla_{\mathbf{r}_j} \frac{f_j}{D_r} \right) \cos \theta_j \delta(x_b - x_j) \right\rangle = 0 \quad (56)$$

because of the angular average. This, however, is not true in the presence of an external potential and hence near the wall. As we now show, this leads to the absence of an equation of state. We consider a model for quorum sensing with

$$f_i(\{\mathbf{r}\}) = f_0 + \frac{f_1 - f_0}{2} \left[\tanh \left(\frac{\tilde{\rho}(\mathbf{r}_i) - \rho_m}{L_f} \right) + 1 \right] \quad (57)$$

$$\tilde{\rho}(\mathbf{r}) = \int d\mathbf{y} K(|\mathbf{r} - \mathbf{y}|) \hat{\rho}(\mathbf{y}); \quad K(r) = Z^{-1} \exp \left[-\frac{1}{1 - r^2} \right] \Theta(1 - r) \quad (58)$$

Here, $\tilde{\rho}(\mathbf{r}_i)$ is a measure of the particle density $\hat{\rho}(\mathbf{r}_i)$ using a coarse-graining kernel K ; Z is a normalisation constant such that $\int d\mathbf{r} K(|\mathbf{r}|) = 1$. The constants f_0 , f_1 , ρ_m and L_f control the dependence of f_i on the local density.

Figure 7 shows the results of simulations of active Brownian particles interacting through (57). The

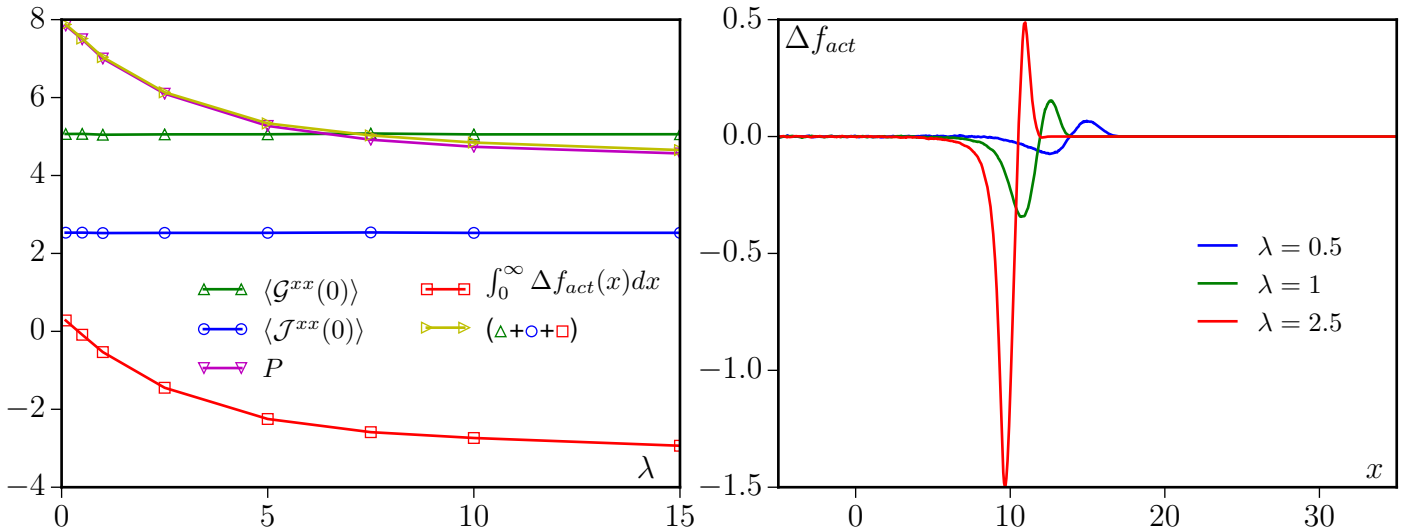


Figure 7. Brownian dynamics simulations of self-propelled disks interacting through Eq. (57) with $f_0 = 4$, $f_1 = 1$, $\rho_m = 2.5$, $L_f = 1.25$, $D_r = 1$, $\tilde{\gamma} = 1$, $m = 1$, $dt = 5 \cdot 10^{-4}$, $D_t = 0$, $\rho_0 = 0.64$, $x_w = 10$. **Left:** The pressure and its different contributions are shown for various wall stiffness. The momentum source Δf_{act} is shown to account for the entire wall dependence of the pressure. **Right:** Steady-state momentum sources $\Delta f_{act}(x)$ for three different wall stiffness.

left panel shows the different terms in the equation for the pressure in Eq. (55) as a function of the wall strength $\lambda = \lambda_R = \lambda_L$ for the potential of Eq. (20). As can be seen the pressure depends on the wall potential and Δf_{act} entirely accounts for this dependence. On the right panel we plot $\Delta f_{act}(x)$ which is non-zero near the walls and depends on the wall potential. As for wall torques, the terms which do not conserve momentum in steady-state account for the breakdown of the equation of state.

2.2. Pairwise forces

We now turn to the case where $f_i(\{\mathbf{r}\}) = f_i$ and consider momentum- and energy-conserving short-range pairwise forces $\mathbf{F}_i(\{\mathbf{r}\})$. This case was already studied in [24]. Our derivation is distinct and we focus here on the role of momentum fluxes. For constant self-propelling forces, Eq. (50) for the local density of active forces reduces to the non-interacting case (28). The expression for the pressure is then:

$$P = \langle \mathcal{J}^{xx}(x_b) \rangle + \langle \mathcal{G}^{xx}(x_b) \rangle + \int_{x_b}^{\infty} \langle \sum_i F_i^x(\{\mathbf{r}\}) \delta(x - x_i) \rangle dx. \quad (59)$$

By the conserving nature of the pairwise forces, Newton's third law implies that the last term in the equation measures the forces across the plane $x = x_b$. Since the forces are assumed to be short ranged this quantity is local. Let us now show this explicitly for the case of conservative pairwise forces

$\mathbf{F}_i(\{\mathbf{r}\}) = -\sum_j \nabla_{\mathbf{r}_i} V(\mathbf{r}_i - \mathbf{r}_j)$. Remembering that Eq. (59) contains an average over y , the last term can be expressed as

$$\int_{x_b}^{\infty} \langle \sum_i F_i^x \delta(x - x_i) \rangle dx = - \sum_{x_i > x_b} \sum_{x_j < x_b} \langle \partial_{x_i} V(\mathbf{r}_i - \mathbf{r}_j) \rangle - \sum_{x_i > x_b} \sum_{x_j > x_b} \langle \partial_{x_i} V(\mathbf{r}_i - \mathbf{r}_j) \rangle, \quad (60)$$

where x_i denotes the x -coordinate of particle i . The second term clearly vanishes so that

$$\int_{x_b}^{\infty} \langle \sum_i F_i^x \delta(x - x_i) \rangle dx = - \langle \sum_{x_i > x_b} \sum_{x_j < x_b} \partial_{x_i} V(\mathbf{r}_i - \mathbf{r}_j) \rangle \quad (61)$$

which can be rewritten in terms of the density-density correlator

$$P_D(x_b) \equiv \int_{x_b}^{\infty} \langle \sum_i F_i^x \delta(x - x_i) \rangle dx = - \int_{w_1 > x_b} d\mathbf{w}_1 \int_{w_2 < x_b} d\mathbf{w}_2 \langle \hat{\rho}(\mathbf{w}_1) \hat{\rho}(\mathbf{w}_2) \rangle \partial_{w_1} V(\mathbf{w}_1 - \mathbf{w}_2), \quad (62)$$

with w_1 (w_2) the x -component of \mathbf{w}_1 (\mathbf{w}_2). $P_D(x_b)$, as stated above, is the force exerted across the $x = x_b$ plane. It is essentially the usual equilibrium contribution from pairwise forces to the pressure, and was identified in active particles in the overdamped regime [14]. All in all, this yield for the pressure

$$P = \langle \mathcal{J}^{xx}(x_b) \rangle + \langle \mathcal{G}^{xx}(x_b) \rangle + P_D(x_b). \quad (63)$$

For short-range interactions, this is a bulk property of the fluid, and hence independent of the wall potential. Note that (63) simply states that the effectively conserved momentum is transferred along the system by both the flux of particles, which carry with them their momentum \mathbf{p}_i and active impulse $\Delta \mathbf{p}_i^a$, and by interparticle forces; this overall momentum is then absorbed by the wall. It is straightforward to extend this derivation to cases with multi-particle conserving forces or to conserving forces which depend on the particles' relative orientations.

3. Momentum sources in motility induced phase separation

One of the most remarkable features of active particles is their generic tendency to phase separate even in the presence of purely repulsive interactions [11, 14, 25, 29–44]. It was recently shown that depending on the type of interactions considered, active particles undergoing MIPS lead to coexisting phases with either equal or unequal mechanical pressures [27]. It is thus natural to probe the mechanical equilibrium between coexisting phases, i.e. ask for the presence or absence of momentum sources at the interface.

For simplicity, in what follows, we focus our discussion on a flat interface between two phases whose direction is normal to the x axis. In this case, the dynamics of the momentum density field (47) leads in steady state to the balance equation:

$$\sum_i \langle f_i(\{\mathbf{r}\}) \mathbf{u}(\theta_i) \delta(\mathbf{r} - \mathbf{r}_i) \rangle + \sum_i \langle \mathbf{F}_i(\{\mathbf{r}\}) \delta(\mathbf{r} - \mathbf{r}_i) \rangle = \nabla \cdot (\langle \mathcal{J}(\mathbf{r}) \rangle) . \quad (64)$$

Its projection on the one-dimensional geometry, obtained as in Eq. (12), is given by

$$\sum_i \langle f_i(\{\mathbf{r}\}) \cos(\theta_i) \delta(x - x_i) \rangle + \sum_i \langle F_i^x(\{\mathbf{r}\}) \delta(x - x_i) \rangle = \partial_x \langle \mathcal{J}^{xx} \rangle \quad (65)$$

As above we consider two representing cases, quorum sensing and pairwise interactions, separately. Before doing so, it is useful to consider the equilibrium case where $f_i = 0$. For concreteness we assume, say, a high density phase at $x < 0$ a low density phase at $x > 0$ with an interface between the two phases in the vicinity of $x = 0$. Integrating Eq. (65) from a point $x_\ell < 0$ to $x_r > 0$, assuming that the distance between x_ℓ and x_r is much larger than both the interaction range and the width of the interface, gives

$$P_D(x_\ell) + \langle \mathcal{J}^{xx}(x_\ell) \rangle = P_D(x_r) + \langle \mathcal{J}^{xx}(x_r) \rangle \quad (66)$$

Namely, by integrating the momentum balance equation over the interface, we obtain the equality of mechanical pressures between the two phases (which each have different values of P_D and $\langle \mathcal{J}^{xx} \rangle$).

We now turn to the two active models.

3.1. Pairwise forces

As we showed before in this case, where $f_i(\{\mathbf{r}\}) = f_i$, an equation of state for the pressure exists. In addition, it is well known that, at coexistence, there is an orientational ordering of the particles at the interface between the two phases [32, 33]. Therefore, naively, the term $\sum_i \langle f_i(\{\mathbf{r}\}) \cos(\theta_i) \delta(x - x_i) \rangle$ in Eq. (65) might lead one to conclude that there are steady-state momentum sources in the system. However, similarly to the ordering at confining walls, this is not the case. In fact, using Eq. (15) and 29 we can rewrite Eq. (65) as

$$\sum_i \langle F_i^x(\{\mathbf{r}\}) \delta(x - x_i) \rangle = \partial_x [\langle \mathcal{J}^{xx} + \mathcal{G}^{xx} \rangle] . \quad (67)$$

This equation implies that the forces between the particles, which in equilibrium systems are compensated only by the momentum flux, are here compensated by both impulse and momentum

fluxes. Repeating the steps leading to Eq. (66) now gives an equality of mechanical pressures between the two phases

$$P_D(x_\ell) + \langle \mathcal{J}^{xx}(x_\ell) + \mathcal{G}^{xx}(x_\ell) \rangle = P_D(x_r) + \langle \mathcal{J}^{xx}(x_r) + \mathcal{G}^{xx}(x_r) \rangle . \quad (68)$$

Despite the presence of a layer of active forces localized at the interface, the mechanical pressures of coexisting phases are equal. This highlights again the effective momentum conservation in this system, as discussed in 1.7, and the absence of momentum sources in steady state.

To illustrate these results we have carried out numerical simulations of self-propelled particles evolving under the dynamics (46) with constant f_i . The interaction force derives from the pairwise repulsive potential

$$V(\mathbf{r}) = \frac{k}{2}(2a - |\mathbf{r}|)^2 \Theta(2a - |\mathbf{r}|) \quad (69)$$

corresponding to harmonic repulsion with stiffness k between disks of radii a . We use periodic boundary conditions in both directions, a high Péclet number known to yield MIPS ($f_i/(\tilde{\gamma}aD_r) = 100$), and a slab geometry that favors vertical phase boundaries. Figure 8 shows that, at steady-state, coexisting phases have equal pressures, in accordance with (68).

3.2. Quorum sensing

We now turn to the case of quorum sensing. Recall that in this case there was no equation of state for the pressure. Using Eq. 50 and Eq. 65, along with the definition given in Eq. 29, we obtain for quorum sensing particles

$$\langle \sum_j \mathbf{v}_j \cdot (\nabla_{\mathbf{r}_j}) \frac{f_i}{D_r} \cos \theta_i \delta(x - x_i) \rangle = \partial_x [\langle \mathcal{J}^{xx} + \mathcal{G}^{xx} \rangle] . \quad (70)$$

At a location x in the interfaces between the coexisting phases the term $\langle \sum_j \mathbf{v}_j \cdot (\nabla_{\mathbf{r}_j}) \frac{f_i}{D_r} \cos \theta_i \delta(x - x_i) \rangle$ is in general non-zero, much like in the vicinity of a confining walls. Moreover, repeating the procedure leading to Eq. 66 now gives

$$\langle \mathcal{J}^{xx}(x_\ell) + \mathcal{G}^{xx}(x_\ell) \rangle + \Delta = \langle \mathcal{J}^{xx}(x_r) + \mathcal{G}^{xx}(x_r) \rangle \quad (71)$$

with

$$\Delta = \int_{x_\ell}^{x_r} \langle \sum_j \mathbf{v}_j \cdot (\nabla_{\mathbf{r}_j}) \frac{f_i}{D_r} \cos \theta_i \delta(x - x_i) \rangle dx = \int_{x_\ell}^{x_r} \Delta f_{\text{act}} dx \quad (72)$$

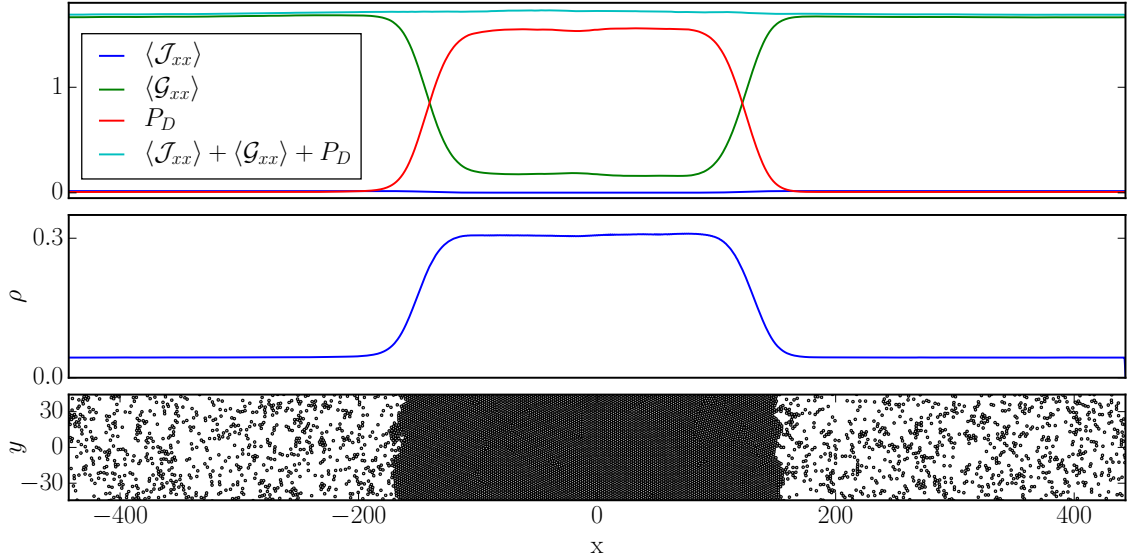


Figure 8. Brownian dynamics simulations of 10000 self-propelled disks with pairwise repulsive forces in a phase separated state. Periodic boundary conditions are used in both directions. The mean packing fraction is $\phi = 0.4$. The repulsive potential is given by Eq. (69) with $a = 1$ and $k = 20$. The other parameters are $f_i = 1$, $D_r = 0.01$, $D_t = 0$, $\tilde{\gamma} = 1$, $m = 1$. Spatial profiles are averaged over 100 persistence times and 100 noise realizations starting from the equilibrated initial configuration shown in the bottom panel. **Top:** Spatial profile of the three contributions to the pressure shown in Eq. (68). Their sum (light blue line) remains constant across phase boundaries. **Middle:** Density profile.

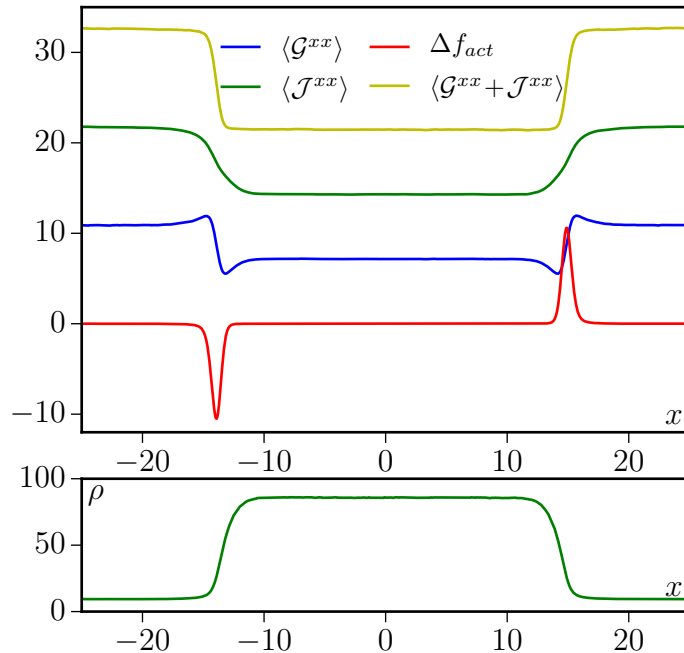


Figure 9. Brownian dynamics simulations of self-propelled disks interacting via (57) and undergoing MIPS. **Bottom:** Density profile averaged along the \hat{y} direction. In the steady-state, we observe the coexistence between a high density phase and a low-density one. **Top:** Steady-state momentum sources and sinks Δf_{act} localized at both interfaces make the sum of momentum and active impulse fluxes $\langle \mathcal{G}^{xx} + \mathcal{J}^{xx} \rangle$ unequal in coexisting phases. Parameters: $f_0 = 4$, $f_1 = 1$, $\rho_m = 25$, $L_f = 12.5$, $D_r = 2$, $\gamma = 1$, $dt = 5 \cdot 10^{-4}$, system size 60×10 .

accounting for the contribution of the steady-state momentum sources localized at the interface. Equation (71) relates the bulk properties of the two phases through \mathcal{J}^{xx} and \mathcal{G}^{xx} . Importantly, the relation involves Δ which depends on the detailed structure of the interface—quite in contrast to the equilibrium case and to the case of active particles interacting via pairwise forces. Once again, we can relate the breakdown of standard mechanical relations to the momentum sources measured by Δf_{act} .

To illustrate these results we have carried out numerical simulations of self-propelled disks interacting via (57) and undergoing MIPS (See Fig. 9). In the steady state, one observes coexisting phases of low and high densities such that Eq. (71) holds: momentum sources and sinks, localized at the interface, make the combined flux of momentum and active impulse $\langle \mathcal{J} + \mathcal{G} \rangle$ unequal in coexisting phases. The lack of effective momentum conservation in the steady-state means that coexisting phases have unequal mechanical pressures, which contrasts with the case of pairwise forces.

4. Conclusion

This paper studies the existence of equations of state for the pressure in dry active systems. Since these systems do not conserve momentum and are out of equilibrium, the existence of an equation of state is far from obvious. In fact, depending on prior biases, one might consider either the existence or absence of an equation of state in such systems to be a surprise. Reference [13] studied several overdamped dry active systems and showed that there is no universal answer: depending on the model, an equation of state may or may not exist. It is therefore natural to ask for the conditions under which an equation of state emerges.

Here, we addressed this question by considering a class of underdamped dry active systems, from which the overdamped limit is easily extracted. The main advantage of the underdamped model is that the momentum field may be studied with ease allowing us to relate the properties of the momentum field and the existence of an equation of state. We show that, generically, the lack of momentum conservation leads to the existence of steady-state momentum sources or sinks near the boundaries of the system which in turn implies that an equation of state for the pressure does not exist. Nonetheless, there is a class of models for which an effective conservation of momentum emerges in the steady state. For this class of

systems, an equation of state exists. The effective momentum conservation can be related to the mean density of active forces being the divergence of the field of active impulse, an observable that measures the momentum a particle will receive on average from the substrate in the future. When the dynamics of the active force leads to a vanishing mean force in the steady state and is independent of the other degrees of freedom, the active impulse is a local quantity, hence leading to an equation of state.

Finally, note that this paper describes only the mechanical properties of the active particles and not the fate of the momentum source from which they are receiving their active impulse. This is relevant for dry systems such as bi-dimensional layers of shaken granulars [26] or any other system in which particles are pushing on a hard boundary [7]. When the active particles exchange momentum with a fluid, we argue that our results extend to the description of osmotic pressure [13,45], although experiments in this case are lacking, as well as explicit treatments from first principles of the coupling between the active particles and the fluid.

Acknowledgments

We thank M. Cates, M. Kardar, A. Morozov, J. Stenhammar for discussions. YF was supported by the NSF, award DMR-1149266, the Brandeis Center for Bioinspired Soft Materials, an NSF MRSEC, award DMR-1420382, and the W. M. Keck Foundation. YF's computational resources were provided by the NSF through XSEDE, award TG-MCB090163, and the Brandeis HPCC. YK is supported by an I-CORE Program of the Planning and Budgeting Committee of the Israel Science Foundation and an Israel Science Foundation grant. AS is funded by the Betty and Gordon Moore foundation. JT was supported by ANR grants Bactterns.

Appendix A. Sufficient condition for the existence of an equation of state

In this appendix we show that if the dynamics of the active force \mathbf{f}_i of particle i does not depend on the other degrees of freedom and leads to a vanishing mean active force in the steady state, then the pressure admits an equation of state. Note that $\langle \mathbf{f}_i \rangle = 0$ in the steady state does not preclude the existence of regions of space in which a local density of active force $\sum_i \mathbf{f}_i \delta(\mathbf{r} - \mathbf{r}_i)$ is non-zero on average. The latter

only relies on correlations between orientations of the particles and their positions.

We consider non-interacting particles evolving according to

$$\dot{\mathbf{r}}_i = \mathbf{v}_i; \quad m\dot{\mathbf{v}}_i = -\tilde{\gamma}\mathbf{v}_i + \mathbf{f}_i - \nabla_{\mathbf{r}_i}V_{\text{ext}} + \sqrt{2\tilde{\gamma}^2D_t}\boldsymbol{\eta}_i. \quad (\text{A.1})$$

We require the evolution of the active force \mathbf{f}_i to be independent of the other degrees of freedom and to be given by an unspecified master equation

$$\dot{P}_i^f(\mathbf{f}_i) = K_i P_i^f(\mathbf{f}_i) \quad (\text{A.2})$$

for the probability $P_i^f(\mathbf{f}_i, t)$ that particle i has a force \mathbf{f}_i at time t . The fact that the dynamics of \mathbf{f}_i is independent of other degrees of freedom means that the operator K_i solely involves \mathbf{f}_i . The joint master equation describing the dynamics of particle i is then given by

$$\dot{P}_i(\mathbf{r}_i, \mathbf{v}_i, \mathbf{f}_i, t) = -\nabla_{\mathbf{r}_i} \cdot [\mathbf{v}_i P_i] - \nabla_{\mathbf{v}_i} \cdot [-\gamma\mathbf{v}_i P_i + \frac{\mathbf{f}_i}{m} P_i - \frac{\nabla_{\mathbf{r}_i} V_{\text{ext}}}{m} P_i - \gamma^2 D_t \nabla_{\mathbf{v}_i} P_i] + K_i P_i \quad (\text{A.3})$$

As before, we define the active impulse through

$$\Delta\mathbf{p}_i^a(\mathbf{r}_0, \mathbf{v}_0, \mathbf{f}_0, t) \equiv \int_t^\infty \overline{\mathbf{f}_i(s)} ds = \int_t^\infty ds \int d\mathbf{f} \mathbf{f} P_i(\mathbf{f}, s | \mathbf{r}_0, \mathbf{v}_0, \mathbf{f}_0, t) \quad (\text{A.4})$$

where $P_i(\mathbf{f}, s | \mathbf{r}_0, \mathbf{v}_0, \mathbf{f}_0, t)$ is the probability of the active force on particle i being \mathbf{f} at time $s > t$, given that the particle was at $\mathbf{r}_i = \mathbf{r}_0$ at time t with velocity $\mathbf{v}_i = \mathbf{v}_0$ and active force $\mathbf{f}_i = \mathbf{f}_0$. Again, $\Delta\mathbf{p}_i^a(\mathbf{r}_0, \mathbf{v}_0, \mathbf{f}_0, t)$ is the total momentum a particle at \mathbf{r}_0 with velocity \mathbf{v}_0 and active force \mathbf{f}_0 will receive, on average, during the rest of its history. Note that the impulse is only finite if the dynamics of \mathbf{f}_i lead to a vanishing mean active force in the steady state, a case to which we restrict our discussion from now on.

We then use the fact that the dynamics of \mathbf{f} are homogenous in time and do not depend on the other degrees of freedom to rewrite (A.4) in the simpler form:

$$\Delta\mathbf{p}_i^a(\mathbf{f}_0) \equiv \int_0^\infty ds \int d\mathbf{f} \mathbf{f} P_i^f(\mathbf{f}, s | \mathbf{f}_0, 0). \quad (\text{A.5})$$

Let us now consider the action of the operator K_i^\dagger on the function $\Delta\mathbf{p}_i^a(\mathbf{f}_0)$:

$$K_i^\dagger \Delta\mathbf{p}_i^a(\mathbf{f}_0) = \int_0^\infty ds \int d\mathbf{f} \mathbf{f} K_i^\dagger P_i^f(\mathbf{f}, s | \mathbf{f}_0, 0) \quad (\text{A.6})$$

$$= \int_0^\infty ds \int d\mathbf{f} \mathbf{f} \partial_s P_i^f(\mathbf{f}, s | \mathbf{f}_0, 0) \quad (\text{A.7})$$

$$\begin{aligned}
&= - \int d\mathbf{f} \mathbf{f} P_i^f(\mathbf{f}, 0 | \mathbf{f}_0, 0) \\
&= - \int d\mathbf{f} \mathbf{f} \delta(\mathbf{f} - \mathbf{f}_0) \\
K_i^\dagger \Delta \mathbf{p}_i^a(f_0) &= - \mathbf{f}_0
\end{aligned} \tag{A.8}$$

Note that K_i^\dagger acts on \mathbf{f}_0 and we used the backward equation to go from (A.6) to (A.7). Then, we consider the evolution of the active impulse of particle i over time, $\Delta \mathbf{p}_i^a(\mathbf{f}_i(t))$. The dynamics of its average is given by

$$\begin{aligned}
\frac{d}{dt} \langle \Delta \mathbf{p}_i^a(f_i(t)) \rangle &= \frac{d}{dt} \int d\mathbf{f}_i \Delta \mathbf{p}_i^a(\mathbf{f}_i) P_i^f(\mathbf{f}_i, t) \\
&= \int d\mathbf{f}_i \Delta \mathbf{p}_i^a(\mathbf{f}_i) K_i P_i^f(\mathbf{f}_i, t) \\
&= \int d\mathbf{f}_i K_i^\dagger \Delta \mathbf{p}_i^a(\mathbf{f}_i) P_i^f(\mathbf{f}_i, t) \\
&= \langle K_i^\dagger \Delta \mathbf{p}_i^a(\mathbf{f}_i(t)) \rangle \\
&= - \langle \mathbf{f}_i(t) \rangle.
\end{aligned}$$

Similarly, we can introduce the field of active impulse density:

$$\Delta \mathbf{p}^a(\mathbf{r}) = \sum_i \Delta \mathbf{p}_i^a(\mathbf{f}_i(t)) \delta(\mathbf{r} - \mathbf{r}_i(t)) \tag{A.9}$$

For non-interacting particles, the joint probability $P(\mathbf{r}_1, \mathbf{v}_1, \mathbf{f}_1, \dots, \mathbf{r}_N, \mathbf{v}_N, \mathbf{f}_N)$ factorizes as

$$P(\mathbf{r}_1, \mathbf{v}_1, \mathbf{f}_1, \dots, \mathbf{r}_N, \mathbf{v}_N, \mathbf{f}_N) = \prod_{i=1}^N P_i(\mathbf{r}_i, \mathbf{v}_i, \mathbf{f}_i) \tag{A.10}$$

so that the dynamics of $\langle \Delta \mathbf{p}^a(\mathbf{r}) \rangle$ are given by:

$$\begin{aligned}
\partial_t \langle \Delta \mathbf{p}^a(\mathbf{r}) \rangle &= \sum_i \int d\mathbf{r}_i d\mathbf{v}_i d\mathbf{f}_i \dot{P}_i(\mathbf{r}_i, \mathbf{v}_i, \mathbf{f}_i) \Delta \mathbf{p}_i^a(\mathbf{f}_i) \delta(\mathbf{r} - \mathbf{r}_i) \\
&= \sum_i \int d\mathbf{r}_i d\mathbf{v}_i d\mathbf{f}_i \Delta \mathbf{p}_i^a(\mathbf{f}_i) \delta(\mathbf{r} - \mathbf{r}_i) [-\nabla_{\mathbf{r}_i} \cdot \mathbf{v}_i P_i(\mathbf{r}_i, \mathbf{v}_i, \mathbf{f}_i) + K_i P_i(\mathbf{r}_i, \mathbf{v}_i, \mathbf{f}_i)]
\end{aligned}$$

Note that the term involving $\nabla_{\mathbf{v}_i}$ in the master equation (A.3) vanishes upon integration over \mathbf{v}_i and that the integrals over the other particles gives $\int d\mathbf{r}_j d\mathbf{v}_j d\mathbf{f}_j P_j(\mathbf{r}_j, \mathbf{v}_j, \mathbf{f}_j) = 1$. Integrating by parts, one then gets

$$\begin{aligned}
\partial_t \langle \Delta \mathbf{p}^a(x) \rangle &= \sum_i \int d\mathbf{r}_i d\mathbf{v}_i d\mathbf{f}_i [-\nabla_{\mathbf{r}} \cdot \mathbf{v}_i \Delta \mathbf{p}_i^a(f_i) \delta(\mathbf{r} - \mathbf{r}_i) P_i(\mathbf{r}_i, \mathbf{v}_i, \mathbf{f}_i) \\
&\quad + P_i(\mathbf{r}_i, \mathbf{v}_i, \mathbf{f}_i) K_i^\dagger \Delta \mathbf{p}_i^a(\mathbf{f}_i) \delta(\mathbf{r} - \mathbf{r}_i)]
\end{aligned}$$

$$\begin{aligned}
&= -\nabla_{\mathbf{r}} \cdot \sum_i \langle \mathbf{v}_i \Delta \mathbf{p}_i^a(\mathbf{f}_i) \delta(\mathbf{r} - \mathbf{r}_i) \rangle + \sum_i \langle K_i^\dagger \Delta \mathbf{p}_i^a(\mathbf{f}_i) \delta(\mathbf{r} - \mathbf{r}_i) \rangle \\
&= -\nabla_{\mathbf{r}} \cdot \langle \sum_i \mathbf{v}_i \Delta \mathbf{p}_i^a(\mathbf{f}_i) \delta(\mathbf{r} - \mathbf{r}_i) \rangle - \langle \sum_i \mathbf{f}_i \delta(\mathbf{r} - \mathbf{r}_i) \rangle
\end{aligned}$$

where we used Eq. (A.8). In the steady state, one thus has

$$\langle \sum_i \mathbf{f}_i \delta(\mathbf{r} - \mathbf{r}_i) \rangle = -\nabla_{\mathbf{r}} \cdot \langle \sum_i \mathbf{v}_i \Delta \mathbf{p}_i^a(\mathbf{f}_i) \delta(\mathbf{r} - \mathbf{r}_i) \rangle = -\nabla_{\mathbf{r}} \langle \mathcal{G} \rangle \quad (\text{A.11})$$

which then leads to an EOS as in section 1.5.

Appendix A.1. Example with multiplicative noise

To illustrate the above results, we consider an active force $\mathbf{f}_i = f_i \mathbf{u}_i(\theta_i)$, where $\mathbf{u}_i(\theta_i) = (\cos \theta_i, \sin \theta_i)$ as in the main text. Position and velocities evolve with Eq. (4). The angle θ_i undergoes rotational diffusion through the following Itô-Langevin dynamics:

$$\dot{\theta}_i = \sqrt{2D_r(\theta_i)} \eta_i. \quad (\text{A.12})$$

which leads to the Fokker-Planck equation

$$\partial_t P_i^f(\theta_i) = \frac{\partial^2}{\partial \theta_i^2} D_r(\theta_i) P_i^f(\theta_i) \quad (\text{A.13})$$

Here, $K_i^\dagger = D_r(\theta_i) \frac{\partial^2}{\partial \theta_i^2}$ so that the impulse can be computed from Eq. (A.8) through

$$\frac{\partial^2}{\partial \theta_i^2} \Delta \mathbf{p}_i^a(\theta_i) = -\frac{f_i}{D_r(\theta_i)} \mathbf{u}(\theta_i) \quad (\text{A.14})$$

which we solve for a given example below.

Following the previous section or directly using Itô calculus, it is easy to show that the dynamics of the density of free active impulse is then given by

$$\partial_t \langle \sum_i \Delta \mathbf{p}_i^a(\theta_i(t)) \delta(\mathbf{r} - \mathbf{r}_i) \rangle = -\langle \sum_i f_i \mathbf{u}(\theta_i(t)) \delta(\mathbf{r} - \mathbf{r}_i) \rangle - \nabla \cdot \langle \sum_i \mathbf{v}_i \Delta \mathbf{p}_i^a(\theta_i(t)) \delta(\mathbf{r} - \mathbf{r}_i) \rangle \quad (\text{A.15})$$

so that, in steady-state, the local force density is given by the divergence of the flux of active impulse

$$\langle \sum_i f_i \mathbf{u}(\theta_i(t)) \delta(\mathbf{r} - \mathbf{r}_i) \rangle = -\nabla \cdot \langle \mathcal{G} \rangle; \quad \mathcal{G} = \sum_i \mathbf{v}_i \Delta \mathbf{p}_i^a(\theta_i(t)) \delta(\mathbf{r} - \mathbf{r}_i). \quad (\text{A.16})$$

For concreteness, we consider

$$D_r(\theta) = \frac{1}{1 + \varepsilon \cos(2\theta)} \quad (\text{A.17})$$

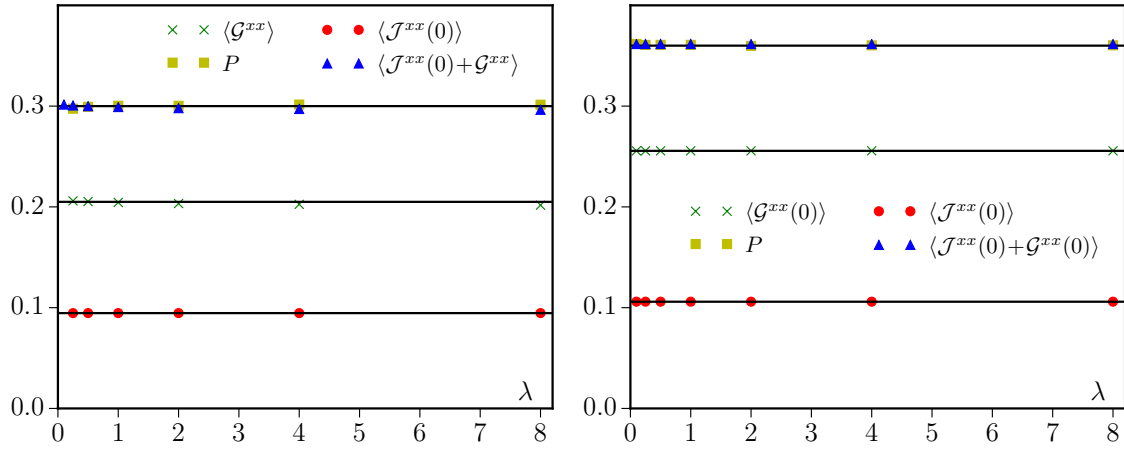


Figure A1. Brownian dynamics simulations of self-propelled disks undergoing dynamics (4) and (A.12) for $m = 1$, $\tilde{\gamma} = 2$, $f_i = 1$, $\rho_0 = 1$, $dt = 5 \cdot 10^{-3}$, $L_x = 20$. Straight lines are guides for the eyes and show that this system also admits an equation of state for the mechanical pressure. To measure $\mathcal{G}^{xx}(0)$, we use Eq. (A.11). **Left:** Here, the active impulses of the particles, $\Delta \mathbf{p}_i^a$, are measured using the definition (A.4) and $\epsilon = 0.2$. **Right:** Here, the active impulse of the particles, $\Delta \mathbf{p}_i^a$, are measured from (A.19) and $\epsilon = 0.4$.

which is such that the steady-state $P(\theta)$ is anisotropic but such that $\langle \mathbf{u}(\theta) \rangle = 0$. Then, the equation for $\Delta \mathbf{p}_i^a(\theta)$ is

$$\partial_{\theta_i}^2 \Delta \mathbf{p}_i^a(\theta_i) = f_i (1 + \epsilon \cos(2\theta_i)) \mathbf{u}(\theta_i) \quad (\text{A.18})$$

whose solution is

$$\Delta \mathbf{p}_i^a = f_i \mathbf{u}(\theta_i) + f_i \frac{\epsilon}{2} \begin{pmatrix} \cos \theta_i + \frac{1}{9} \cos 3\theta_i \\ -\sin \theta_i + \frac{1}{9} \sin 3\theta_i \end{pmatrix} \quad (\text{A.19})$$

Fig A1 shows that, indeed, the pressure is given in this case by $P = \langle G^{xx}(x_b) + J^{xx}(x_b) \rangle$ with $x_b = 0$, hence satisfying an equation of state: it is independent of the stiffness of the confining potential.

-
- [1] Marchetti M C, Joanny J F, Ramaswamy S, Liverpool T B, Prost J, Rao M and Aditi Simha T B 2010 *Reviews of Modern Physics* **85** 1143–1189
 - [2] Julicher F, Kruse K, Prost J, and Joanny J F 2007 *Physics Reports* **443** 3
 - [3] Narayan V, Ramaswamy S and Menon N 2007 *Science* **317** 105–108
 - [4] Deseigne J, Dauchot O and Chate H 2010 *Physical Review Letters* **105** 9
 - [5] Palacci J, Cottin-Bizonne C, Ybert C and Bocquet L 2010 *Physical Review Letters* **105** 088304
 - [6] Galajda P Keymer J C P and R A 2007 *J. Bacteriol* **189** 1033

- [7] Bricard A, Caussin J B, Desreumaux N, Dauchot O and Bartolo D 2013 *Nature* **503** 95–98
- [8] Di Leonardo R, Angelani L, DellafArciprete D, Ruocco G, Iebba V, Schippa S, Conte M, Mearini F, De Angelis F and Di Fabrizio E 2010 *Proceedings of the National Academy of Sciences* **107** 9541–9545
- [9] Yang X, Manning M L and Marchetti M C 2014 *Soft Matter* **10** 6477 ISSN 1744-683X URL <http://xlink.rsc.org/?DOI=C4SM00927D>
- [10] Mallory S, Valeriani C and Cacciuto A 2014 *Physical Review E* **90** 032309
- [11] Takatori S, Yan W and Brady J 2014 *Physical Review Letters* **113** 028103 ISSN 0031-9007 URL <http://link.aps.org/doi/10.1103/PhysRevLett.113.028103>
- [12] Fily Y, Baskaran A and Hagan M F 2014 *Soft Matter* **10** 5609–5617 ISSN 1744-683X
- [13] Solon A P, Fily Y, Baskaran A, Cates M E, Kafri Y, Kardar M and Tailleur J 2015 *Nat Phys* **11** 673–678 ISSN 1745-2473
- [14] Solon A P, Stenhammar J, Wittkowski R, Kardar M, Kafri Y, Cates M E and Tailleur J 2015 *Phys. Rev. Lett.* **114**(19) 198301
- [15] Ginot F, Theurkauff I, Levis D, Ybert C, Bocquet L, Berthier L and Cottin-Bizonne C 2015 *Physical Review X* **5** 011004
- [16] Takatori S C and Brady J F 2015 *Physical Review E* **91** 032117 ISSN 1539-3755 URL <http://link.aps.org/doi/10.1103/PhysRevE.91.032117>
- [17] Yan W and Brady J F 2015 *Journal of Fluid Mechanics* **785** R1
- [18] Yan W and Brady J F 2015 *Soft Matter* **11** 6235–6244
- [19] Winkler R G, Wysocki A and G G 2015 *Soft Matter* **11** 6680–6691
- [20] Speck T and Jack R L 2016 *Physical Review E* **93** 062605
- [21] Nikolai N, Solon A P, Kafri Y, Kardar M, Tailleur J and R V 2016 *Physical Review Letters* **117** 098001–5
- [22] Joyeux M and Bertin E 2016 *Physical Review E* **93** 032605
- [23] Falasco G, Baldovin F, Kroy K and Baiesi M 2016 *New Journal of Physics* **18** 093043
- [24] Steffenoni S, Falasco G and Kroy K 2016 *arxiv:1612.08404*
- [25] Marchetti M C, Fily Y, Henkes S, Patch A and Yllanes D 2016 *Current Opinion in Colloid & Interface Science* **21** 34–43 ISSN 1359-0294
- [26] Junot G, Briand G, Ledesma-Alonso R and Dauchot O 2017 *arxiv:1703.04195*
- [27] Solon A P, Stenhammar J, Cates M E, Kafri Y and Tailleur J 2016 *arXiv preprint arXiv:1609.03483*
- [28] Irving J and Kirkwood J G 1950 *The Journal of chemical physics* **18** 817–829
- [29] Cates M E and Tailleur J 2015 *Annu. Rev. Condens. Matter Phys.* **6** 219–244
- [30] Tailleur J and Cates M 2008 *Physical review letters* **100** 218103
- [31] Thompson A, Tailleur J, Cates M and Blythe R 2011 *Journal of Statistical Mechanics: Theory and Experiment* **2011**

P02029

- [32] Fily Y and Marchetti M C 2012 *Physical review letters* **108** 235702
- [33] Redner G S, Hagan M F and Baskaran A 2013 *Physical review letters* **110** 055701
- [34] Bialké J, Löwen H and Speck T 2013 *EPL (Europhysics Letters)* **103** 30008
- [35] Stenhammar J, Tiribocchi A, Allen R J, Marenduzzo D and Cates M E 2013 *Physical review letters* **111** 145702
- [36] Buttinoni I, Bialké J, Kümmel F, Löwen H, Bechinger C and Speck T 2013 *Physical review letters* **110** 238301
- [37] Wysocki A, Winkler R G and Gompper G 2014 *EPL (Europhysics Letters)* **105** 48004
- [38] Theurkauff I, Cottin-Bizonne C, Palacci J, Ybert C and Bocquet L 2012 *Physical review letters* **108** 268303
- [39] Wittkowski R, Tiribocchi A, Stenhammar J, Allen R J, Marenduzzo D and Cates M E 2014 *Nature communications* **5** 4351
- [40] Speck T, Bialké J, Menzel A M and Löwen H 2014 *Physical Review Letters* **112** 218304
- [41] Matas-Navarro R, Golestanian R, Liverpool T B and Fielding S M 2014 *Physical Review E* **90** 032304
- [42] Zöttl A and Stark H 2014 *Physical review letters* **112** 118101
- [43] Suma A, Gonnella G, Marenduzzo D and Orlandini E 2014 *EPL (Europhysics Letters)* **108** 56004
- [44] Redner G S, Wagner C G, Baskaran A and Hagan M F 2016 *Physical Review Letters* **117** 148002
- [45] Rodenburg J, Dijkstra M and van Roij R 2016 *arXiv preprint arXiv:1609.08163*